Load-Aware Modelling in Cellular Networks with Repulsively Deployed Base Stations

By

Ahsan Ali

A thesis submitted to Macquarie University
for the degree of Master of Research
Department of Engineering
9 October 2015

Except where acknowledged in the customary manner, the material presented in this thesis is, to the best of my knowledge, original and has not been submitted in whole or part for a degree in any university.

Ahsan Ali

Acknowledgments

Foremost I would like to thank my supervisor Dr. Rein Vesilo for his continual support and guidance over the past year. His seemingly boundless energy, commitment and loyalty to students has been truly inspirational. Dr. Vesilo has always encouraged me to think independently and listened patiently to my ideas. His emphasis on clarity and mathematical rigor in my work has helped me a lot in achieving my academic goals. I couldn't have had a better supervisor.

I am extremely grateful to Macquarie University for providing me with the complete financial support and all the facilities required for the completion of my Masters of Research.

I also want to thank my friends Affan, Noman, Shayan, Tariq and Usman for making my stay here a memorable one. Special thanks to Usman for cheering me up and providing me the motivation whenever I felt sad during the first few weeks of my stay here in Macquarie University.

Finally, I shall forever be grateful to my mother, brothers and sister. Needless to say, this work would not have been accomplished without their constant love, support and continuous encouragement. With this I would also like to take the opportunity to thank Skype$^{\mathsf{TM}}$, I really never felt "away" from home!

Abstract

Spatial models for the locations of base stations (BSs) in cellular networks have long been desirable since they play a pivotal role in evaluating the mutual interference and, hence, overall performance of the network. The Poisson point process (PPP) is the most analytically tractable and widely used model for the location of BSs, but it fails to capture the underlying separation between BSs of cellular networks. This thesis uses most recently proposed model, the Ginibre point process (GPP), for the location of BSs to capture the underlying separation between them. The GPP is a special type of determinantal point process (DPP) that provides the best fit for the random phenomena where repulsion exists and at the same time maintains the analytical tractability of the analysis.

Apart from spatial models for the location of BSs, another most important aspect is the BS load which has not been addressed in most of the previous analyses. The main emphasis of this thesis is to incorporate the BS load using the idea of conditional thinning of the interference field. For a single-tier cellular network where the BSs are spatially distributed via GPP and transmitting with a certain probability, we derive the coverage probability for the typical user under the assumption of a Rayleigh fading channel. To evaluate the coverage, we have also determined the Laplace transform of interference, under the diagonal approximation, in a GPP-based model that can be used for various other settings as well. In addition, to show that the β-GPP model is accurate for cellular networks, we provide the fitting results of β-GPP to that of actual BS deployment data set in terms of the coverage probability. We also model the multi-tier cellular network using the β-GPP and provide the Monte Carlo simulation results for the coverage probability under various network settings.

Contents

4   Modelling Multi-Tier Cellular Networks   44

5   Conclusion and Future Work   52

Bibliography   55

List of Figures

Chapter 1

Introduction

The history of communication goes back to centuries where messengers were used to transport the messages. These messengers may walk or use boat, horse or some other means to carry messages from one place to another. Some sort of fire, smoke or other signals were also used to carry the predefined messages. But with the advancement of technologies these mediums were replaced by mechanical telegraphs in 1794, by copper wires in 1837, by electromagnetic waves in 1896 and by optical fibres in 1973 [1]. The remarkable work of Guglielmo Marconi in 1896 on electromagnetism, in which he transmitted a wireless signal at about 2 km, has started the new era of wireless communications. Since then, the radio technology keeps on evolving.

1.1   Cellular Networks

The design concept of early radio technology was to cover the as much area as possible using a high power transmitter separated by larger distances. This methodology causes the system to not reuse the same frequency even at larger distances and thus creating the capacity problem [2]. The major breakthrough to overcome the problem of capacity came from the concept of cellular networks in 1970's where the main idea was to replace the high power transmitters with many lesser power transmitters, known as base stations (BSs), and reuse the same frequency when it gets attenuated at farther distance. This attenuation is termed as *distance-based path loss*. Based on this distance-based path loss the coverage area of a single BS is defined and is referred to as *cell* and all the cells are connected via wired or wireless connection to each other. The resulting network, known as *cellular network*, is the main focus of this thesis.

Cellular networks were primarily designed to carry voice but with the passage of time, due to proliferation of advance communication devices like smart phones, laptops, tablets have led to a paradigm shift in the way these networks are perceived and deployed. As per

white paper [3], released by cisco, existing networks will not be able to meet the demands of users by 2020. A straight forward calculation reveals that around a $1000\times$ increase in capacity is required to meet the crushing demands of users and applications over a decade. This has in fact been also acknowledged as the main challenge by the major cellular companies e.g., by Qualcomm's "$1000\times$ challenge"[1].

Traditional ways of increasing the capacity like better modulation schemes, medium access algorithms etc. will not be able to meet this challenge, since most of the technologies are already running at their maturity level. The increase in capacity at such a rapid rate requires some fundamental changes in the cellular networks and several research efforts in academia and industry have been made to meet this $1000\times$ challenge, see [4]. According to authors in [5], big three wireless technologies to cope up with this data deluge are mm-waves (adding more spectrum), massive-MIMO (increasing number of antennas) and ultra-densification (deploying more BSs).

1.2   Multi-tier Cellular Network

In response to the capacity challenges, the standardization bodies are developing new solutions to accommodate the increased capacity demand. One promising solution is the addition of small cells [6] to already existing cellular networks. These small cells are already the part of 3G, LTE and WiMAX standards, and many cellular service providers have already launched their small cell services [7]. The resulting network constituted by traditional cellular network overlaid by small cells is called a *multi-tier cellular network* (also referred to as heterogeneous network [HetNet]).

Small cell is an umbrella term used for low-powered and cost-effective wireless access points that operates in both licensed and unlicensed band. The term small cell covers femtocells, picocells, microcells and metrocells which may or may not be operated and owned by cellular network operators. Figure 1.1 provides the illustration of a 3-tier cellular networks consisting of macro, pico and femto cells. Each tier in the network is distinguished based on its transmit power, base station density and data rate.

Small cells provide a very fine grained and customer needs-oriented network expansion, which allows an optimized network operation. Cellular operators normally install the small

---

[1]https://www.qualcomm.com/invention/technologies/1000x
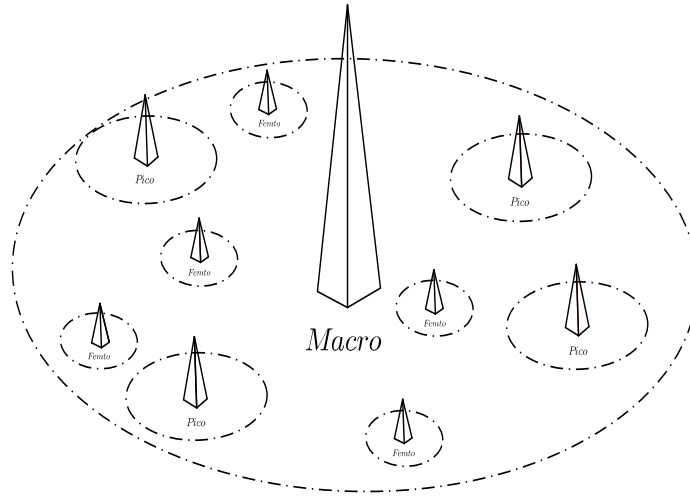
Figure 1.1: Illustration of a 3-tier cellular network consisting of macro, pico and femto cells. Only a single macro cell is shown for the sake of simplicity.

cells in no coverage regions or at the cell edges of BSs to provide the high data rates to their users. On the other hand, some of the small cells are deployed and managed by the users to get the guaranteed Quality of Service (QoS). In this way, the cellular operators enjoy the reduced capital expenditure (CapEx) and operational expenditure (OpEx). Small cells also offload a controllable amount of user and their associated traffic from the congested macro BSs.

Since some of the small cells are installed by the users, the owner of that particular small cell may not want it to be accessed by other users in the network. Based on this access mechanism small cells can be divided into three main categories namely *open access*, *closed access* and *hybrid access* [6]. In case of an open access, the small cell is available to all the users in the network. On the other hand, closed access small cells allow only a subset of users to connect, often called as closed subscriber group (CSG). Therefore, the close access small cells generally degrade the performance of the overall network [8]. In order to maintain a balanced trade off between overall performance of the network and QoS, hybrid access is considered to be a potential solution. In hybrid access the available spectrum is divided into two groups. One group is assigned to CSGs and other one to the non-subscribers. In this way QoS will be guaranteed while maintaining the overall performance of the network.

1.2.1   Interference Modelling

Due to the scarcity of the wireless spectrum, universal frequency reuse is one of the main characteristics of multi-tier cellular networks [9], [10]. That is, the available wireless spectrum will be aggressively reused by all the tiers in the network. The obvious drawback of this type of frequency reuse is the increased interference which may deplete the achieved capacity gains. In case of multi-tier cellular networks with K coexisting tiers there are two types of interference:

- *co-tier (or intra-tier):* The interference experienced by a user served by a BS of tier i from the other BS of the same tier. For instance, the interference experienced by a user in a single-tier macro network.

- *cross-tier (or inter-tier):* The interference experienced by a user served by BS of tier i from the BS of tier j, $\forall j \neq i$ j, $i = 1, 2, 3, \cdots K$.

In multi-tier cellular networks interference is the major performance limiting factor since it directly affects the coverage regions. A user standing in front of the BS may not get coverage due to interference caused by other BSs. Understanding the spatial patterns of co- and cross-tier interference under the various network configurations are of primary interest to both the academics and industry communities.

Interference modelling has always been a challenging problem in the cellular networks because of its dependency on the location of the BSs. Traditional ways of interference characterization in the single-tier cellular networks includes the extensive simulations [11] by assuming that BSs follows the regular grid structure. However, due to the variation of the capacity demands across the service area, the BSs will not follow the exact grid-based model, in fact they are becoming more random. Another important aspect which affects the interference patterns is the BS load. This is because of the fact that some of the BS in the network may not transmit in specific time slot and thus do not contribute towards interference. So, apart from the locations of the transmitters the load of each BS is also important to characterize the overall spatial distribution of interference in the network.

Just like single-tier cellular networks, multi-tier cellular networks will have more topological randomness because of the addition of small cells (e.g. femto cells) randomly installed by the users. The effect of BS load in case of multi-tier cellular is more promi-

nent since small cells have very less number of users connected to it and may not be transmitting most of the time. Apart from small cells load, another important aspect is the access policy since under closed access policy the subscriber may not be able to connect to the small cell but still getting the interference from that particular small cell.

As mentioned earlier, traditionally the locations of BSs in a finite region are assumed to follow a regular hexagon grid structure for the analyses of cellular network. But, this approach is not justified in future cellular networks. Recently, a new modelling approach based on stochastic geometry and random graphs has been adopted for the analyses of wireless networks with random topologies. Stochastic geometry analyses not only capture the topological randomness in the location of transmitters in the networks but also leads to tractable analytical result [12].

1.3   Aims and Scope

Since the topology of the cellular networks is becoming more and more random which has direct impact on the spatial distribution of interference in network. This thesis aims at using tools from stochastic geometry to study the spatial distribution of interference in cellular networks. While using the random point processes (PPs) for the locations of BSs in cellular networks the main concern is how accurately the selected PP models the actual BS deployment scenario. In case of single-tier cellular networks the spatial distribution of BSs exhibit some regularity due to the careful frequency planning by the operator. So, the PPs which exhibit repulsion in between the different points are the main focus of this thesis.

In this work we first aim at exploring various PPs that accurately model the separation between the BSs in a single-tier cellular network. In this direction, based on the fair balance between the analytical tractability, modelling accuracy and practicability of a PP, specific PP would be selected for the interference analysis in cellular networks. To render the more practical analysis this work also aims at incorporating the BS load in the analysis.

For a single tier cellular network with repulsively deployed BSs, transmitting with certain probability in the specific time slot, the mathematical model for coverage probability is the main scope of this work. The extension of the same mathematical analysis to multi-tier cellular network does not come under the scope of this work and left as a

future work. However, we are aiming to model the multi-tier cellular network using PPs and provide the numerical analysis under various network settings.

1.4   Organization and Main Contributions

The organization of this work is as follows. The thesis can be divided into three distinct, yet related parts. First part deals with the exploration of different repulsive PPs that can be used for the modelling of cellular networks. Various stochastic geometry tools that are essential for the analysis of PPs are also discussed. In the second part we study the single-tier cellular network where the locations of BSs are taken from β-Ginibre point process(β-GPP). Here we also incorporate the notion of BS load in the analysis. The final part deals with the simulations of multi-tier cellular networks where each tier of the network is modelled by tuning the parameter β of the β-GPP model. This part also contains the results for the modelling accuracy of the β-GPP model for the real world scenario. The main contributions of this work are as follows:

1) Though the spatial arrangement of BSs in cellular networks is taken to be a Poisson point process (PPP) in most of the previous analyses, this assumption is impractical because of the regularity in the location of BSs in the real world scenario. Another assumption in most of the previous work is all the BSs are transmitting at all the times which is not the case in the real world scenario. Chapter 3 addresses both of these points where we have used the β-GPP to model the location of BSs and incorporated the notion of BS load in the analysis. Specifically, we derive the expression for the coverage probability– the probability that the received signal power is greater than certain threshold– for a single-tier cellular network when all the BSs are not transmitting in the specific time slot.

2) If the received signal power in wireless networks is exponentially distributed, i.e., Rayleigh fading channel, the coverage (success) probability is given by the *Laplace Transform* of interference. In this work we also provide the upper bound on the Laplace transform of interference in a β-GPP configured single-tier cellular network.

3) The extension of single-tier model to the multi-tier cellular network using β-GPP is another major contribution of this thesis. Numerically, we have provided the coverage analyses for the typical user when all the BSs in different tiers are transmitting with certain probabilities. The effect of access policies of small cells is also investigated in this work.

Chapter 2

Stochastic Geometry

2.1 Introduction

Random geometrical patterns occur in many fields of science and technology and are often modelled by the PPs and require some statistical analysis. Some of the main examples include environmental sciences, ecology, geography, astrophysics, fisheries and forestry. Statistical analysis of such random data set require some sophisticated methods from probability and statistics. The branch of mathematics which deals with the statistical analysis of such random patterns is known as *Stochastic Geometry* [13]. Recently there has been an increased interest in using stochastic geometry tools for the analysis of wireless networks [14] because of the random distribution of BSs in the specific region. In this chapter we provide the detailed overview on the models and tools that can be used for the analysis of the cellular networks.

In many actual cellular networks, two BSs are forbidden to be closer to each other than a certain minimum distance. This is mainly because of the fact that the cellular network operator installs BSs after careful frequency planning which induces some separation in between them. So, the spatial PPs where nearby points repel each other are desirable for modelling the cellular networks. The main objective of this chapter is to describe the PPs that can be used for the modelling of cellular networks. The main emphasis is on the determinantal point processes (DPPs) since these PPs are used for the modelling of cellular networks in this thesis. Some of the main stochastic geometry tools that can be used for the analysis of PPs are also defined in this chapter. For further details on probability theory and stochastic geometry readers are requested to see [13–15].

2.2   Point Process

Informally, a PP Φ on $\mathbb{R}^d$ is a random variable which take values from the set of simple and finite sequences N, where N is the set of all sequences of points in $\mathbb{R}^d$ such that any sequence $\phi \in \mathsf{N}$:

- has only a finite number of points in any bounded subset B of $\mathbb{R}^d$
- has no two overlapping points, i.e., "*simple*"

Formal definition of PP can be well understood by its relation to a real-valued random variable which is defined below.

Definition 1. *Let X be a real-valued random variable on the probability space $(\Omega, \mathcal{A}, \mathbb{P})$, i.e., an $\mathcal{A}$-measurable function $X : \Omega \to \mathbb{R}$. The distribution of X is the measure*

$$F \triangleq \mathbb{P} \circ X^{-1}, \tag{2.1}$$

on $(\mathbb{R}, \mathcal{B})$, where $\mathcal{B}$ is the Borel sigma algebra of $\mathbb{R}$, defined by

$$F(B) = \mathbb{P} \circ X^{-1}(B) = \mathbb{P}(X \in B) \quad \forall B \in \mathcal{B}. \tag{2.2}$$

So measurability is the requirement that $(X^{-1}(B) \in \mathcal{A}) \, \forall \, B \in \mathcal{B}$.

Definition 2. *(Point Process) Formally, for any probability space $(\Omega, \mathcal{A}, \mathbb{P})$, PP Φ can be defined as a measurable mapping from $(\Omega, \mathcal{A}, \mathbb{P})$ to $(\mathsf{N}, \mathcal{N})$ i.e.,*

$$\Phi : \Omega \to \mathsf{N}. \tag{2.3}$$

So a PP is a random variable that takes values in the set of sequences N. Each outcome $\omega \in \Omega$ determines an entire point sequence $\Phi(\omega)$. The distribution of Φ is given by:

$$\mathbf{P}(E) = \mathbb{P} \circ \Phi^{-1}(E) = \mathbb{P}(\Phi \in E) \quad \forall E \in \mathcal{N}. \tag{2.4}$$

In this case measurability requires that $\Phi^{-1}(E) \in \mathcal{A}$. Here $\mathcal{N}$ is the smallest sigma algebra so that maps $\phi \to \phi(B)$ are measurable, and $\phi(B)$ denotes the number of points of ϕ in $B \subset \mathbb{R}^d$.

Repulsive Point Process	Complete Spatial Random	Attractive Point Process
▸Matern hard-core	Poisson Point Process (PPP)	▸Poisson cluster process
▸Gibbs process	Binomial Point Process (BPP)	▸Neyman-Scott process
▸Perturbed lattice		▸Metern cluster process
▸Determinantal point process		▸Thomas cluster process
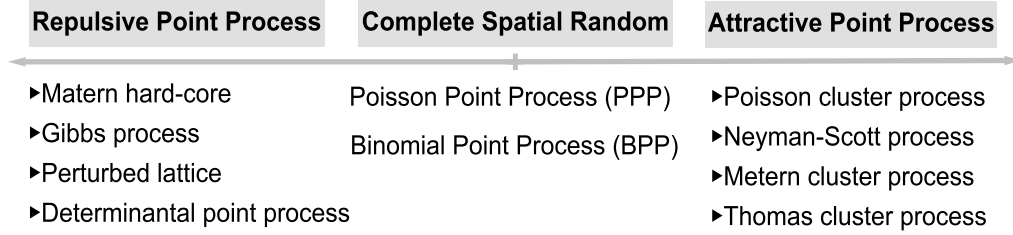
Figure 2.1: Point process taxonomy: The PPP is the the complete spatial random (CSR) model with zero interaction between the points. On moving to the left on the axis, points start to repel each other whereas points tend to attract each other on the other side of the axis.

There are various ways by which a PP can be represented. Using *random set formalism* [14], a PP Φ can be described as

$$\Phi = \{x_1, x_2 \cdots x_n\} \subset \mathbb{R}^d, \tag{2.5}$$

where $x_i \in \mathbb{R}^d$ takes the values from some probability space $(\Omega, \mathcal{A}, \mathbb{P})$.

Based on the correlation between the points of a PP, PPs can be divided into two main categories, i.e., *attractive* and *repulsive*. Figure 2.1 provides the taxonomy of these two main categories of PPs. The most simplest PP without any dependency in between the points is PPP also referred to as Complete Spatial Random (CSR). Although the PPP is CSR process but it serves as the underlying process for most of the repulsive and attractive PPs. In the following section we provide a brief overview on the PPP.

2.2.1 Poisson Point Process

A stationary PPP of density λ can be characterized by the following two properties:

- The number of points in any set $B \subset \mathbb{R}^d$ is a Poisson random variable with mean $\lambda|B|$.

- The number of points in any disjoints sets are independent random variables.

From definition we can write

$$\mathbb{P}(\Phi(B) = k) = \exp(-\mu)\frac{\mu^k}{k!}, \tag{2.6}$$

where μ is the mean number of points i.e., $\lambda|B|$.

PPP exhibits some unique properties [13] which makes the analysis tractable, some of which are

- *Stationarity:* A PP $\Phi = \{x_i\}$ is said to be stationary if

$$\mathbb{P}(\Phi \in Y) = \mathbb{P}(\Phi_a \in Y), \tag{2.7}$$

  for all $Y \in \mathcal{N}$, where $\mathcal{N}$ is the smallest sigma algebra and $\Phi_x = \{x_n + a\}$.

- *Isotropic:* A PP $\Phi = \{x_i\}$ is said to be isotropic if

$$\mathbb{P}(\Phi \in Y) = \mathbb{P}(\Phi \in \mathsf{r}Y), \tag{2.8}$$

  where r is the rotation in the space.

- *Motion Invariance:* A PP Φ which is both stationary and isotropic is known as motion invariant PP.

- *Slivnyak's theorem:* applies to it, which means that conditioning on a certain point does not change the overall distribution of the process unlike all other PPs.

- *Independent Thinning* of a PPP of intensity λ (i.e., retaining some points with probability p independent of other points and discarding with probability $(1 - p)$) results in two independent PPPs with intensity $p\lambda$ and $(1 - p)\lambda$, respectively.

- *Superposition* of two independent PPPs with intensities λ_1 and λ_2 results in a single PPP with intensity $\lambda = \lambda_1 + \lambda_2$.

Due to the above mentioned properties, the PPP model is the most analytically tractable and the most popular model used in the literature. PPP has been used to model large scale wireless scale ad hoc networks for more than three decades and the performance of such networks have been well characterized and understood. Most of the results in case of wireless ad hoc networks, modelled via PPP, have been well summarized in two monographs [16] and [17]. The independent assumption of PPP can be justified to model the wireless ad hoc networks but for the case of cellular networks BSs are not independent of each other. As it can be seen easily from Figure 2.2 that in some areas the points tends to cluster leaving behind some gaps in other regions which is not the case with the cellular networks.
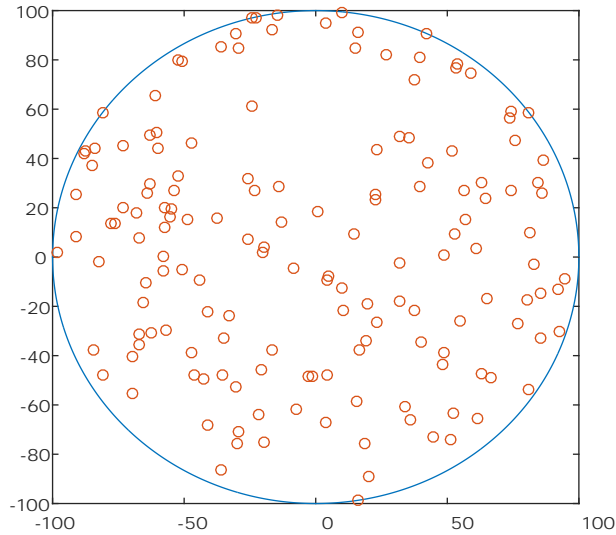
Figure 2.2: Realization of PPP with intensity $\lambda = 0.005$ in the ball of radius 100 meters centred at origin i.e., $b(o, 100)$

2.2.2 Binomial Point Process

The binomial point process is a basic process whereby fixed number of nodes n are uniformly and independently distributed in the compact subset $W \subset \mathbb{R}^d$. Formally BPP can be defined as follows:

Definition 3. *Let $\Phi = \{x_1, x_2 \cdots\} \subset W$ be a point process with a fixed number* n *of nodes in a compact set W. Φ is a BPP if* n *nodes are uniformly and randomly distributed in the compact set W.*

Due to independence assumption BPP are widely used to model the ad hoc network. [18] has found the probability density function for the nearest neighbor when points are distributed via BPP.

In the following section we describe the PPs in which points are negatively correlated and can be used as the potential candidates for the modelling of cellular networks.

2.3 Repulsive Point Processes

Repulsive PPs can be generally categorized as hard-core or soft-core processes. A hard-core process occurs by ensuring a minimum positive distance between any two points, whereas in soft-core processes two points can be closer to each other i.e., they exhibits

weak repulsive force between points. Some of the main repulsive PPs that can be used for the modelling of cellular networks are described below.

2.3.1   Matérn Hard-Core Process

The Matérn hard-core process is generated by *dependent thinning* of a homogeneous PPP to ensure the minimum separation between any two points. Based on the type of thinning these PPs can further be divided in two main types [14], explained below.

1. **Matérn Hard-Core Process of type I:** Using the underlying PPP Φ_b with intensity λ_b, first flag for removal all points that have a neighbour within distance r. Then remove all flagged points. The intensity of the remaining points in 2-dimensional Euclidean space is then given by [14] as

$$\lambda = \lambda_b \exp(-\lambda_b \pi r^2). \qquad (2.9)$$

2. **Matérn Hard-Core Process of type II:** Starting with a homogeneous PPP Φ_b with intensity λ_b, add an independent mark to each point x, uniformly distributed on $[0, 1]$. Flag for removal all points that have a neighbour within distance r that has a smaller mark. Then remove all the flagged points. The intensity of remaining points in 2-dimensional Euclidean space is then given by [14] as

$$\lambda = \frac{1 - \exp(-\lambda_b \pi r^2)}{\pi r^2}. \qquad (2.10)$$

It can be observed from the above definitions that these PPs maintain the minimum distance in between the points. They have the capability of providing the best fit for the cellular networks. In literature, these PPs have been extensively used to model the concurrent transmission in CSMA networks [19]. [20] has made the first effort to model the cellular networks using these PPs, the authors in this paper used coverage probability to fit these PPs to actual BS data set. Based on the analysis, it was found that these PPs provide the best fit to single-tier cellular network but unfortunately they exhibit some properties which makes them analytically intractable.

2.3.2 Gibbs Model

Gibbs processes are constructed on the basis of probability densities. The main idea is to shape the distribution of the basic PP, usually a PPP, using the density function $f(\varphi)$ on the space of counting measures ζ. The density function is also called the *likelihood* function.

In order to formally define the Gibbs process suppose:

- $f(\varphi)$ is a function such that $f(\varphi) > 0 \Rightarrow f(\varphi') > 0 \quad \forall \varphi' \subset \varphi$,
- Q is the distribution of a PPP with intensity $\lambda = 1$.

Regarding φ as a counting measure we have $\int_\zeta Q \, d(\varphi) = 1$. If $\int_\zeta f(\varphi)Q(d\varphi) = 1$, then the probability measure $\mathbb{P}(Y)$ on the measurable space $(\zeta, \mathcal{N})$ that satisfies $\mathbb{P}(Y) = \int_Y f(\varphi)Q(d\varphi) \quad \forall Y \in \mathcal{N}$, is the distribution of Gibbs process. The important type of Gibbs process is the Strauss process which has been used in the literature.

Definition 4. *(Strauss Process) The Strauss process is a special type of Gibbs process with density function $f : \zeta \mapsto \mathbb{R}^+$ given by*

$$f(\varphi) = ca^{\varphi(\mathbb{R}^2)} \exp(-bt_{\tilde{R}}(\varphi)), \tag{2.11}$$

where $\tilde{R}$ is called the interaction radius, b determines the strength of repulsion between the nodes, and $t_{\tilde{R}}(\varphi)$ denotes the number of point pairs $\{x, y\}$ in φ such that $||x - y|| < \tilde{R}$. Unlike Matérn hard-core process Strauss process is the soft core process, i.e., the repulsion between the points is not strict, two points can coexist within close proximity. [20] has also used the Strauss process, the other being the hard core process, for fitting to the actual BS data set. The authors in [20] have further commented that while being accurate they are highly intractable for the detailed analysis of the cellular networks.

2.4 Determinantal Point Process

The formal notion of DPPs was first introduced by O. Macchi in 1975 [21] for the modelling of fermions in quantum mechanics. Before that, they were extensively used in the random matrix theory, mathematical physics and combinatorics. Apart from this, these PPs have also been used in the fields of biology, ecology and forestry, see [22] for

detailed discussion. Recently these PPs have been proposed to model the wireless networks due to the fact that their moments are explicitly known, parametric families can easily be considered and their densities on any compact sets admit a closed form expression [23]. The authors in [22] provided a detailed discussion on the above mentioned properties and also showed that these PPs are analytically tractable unlike other repulsive PPs (Gibbs processes and Matérn hard-core processes). DPPs have very appealing properties in contrast with other repulsive PPs, some of the which, as mentioned in [22], are listed below

- Uniqueness of the DPP is ensured when it exists.
- All orders of moments are described by certain determinants of the kernel matrix K.
- The restriction of a DPP to a compact subset S of the space is also a DPP with its distribution specified by the restriction of K to $S \times S$.
- The density of a restricted DPP is given by a normalizing constant times the determinant of a matrix with entries given by the restricted kernel.
- The spectral representation can be approximated by Fourier series.
- DPP can be easily simulated.

Like PPP, DPPs are also motion invariant, independent thinning of DPP is also a DPP [22, Appendix A], reduced Palm measure of a DPP is also a DPP [22, Appendix C]. We will discuss these properties in detail later in the chapter. Due to these properties and repulsive nature DPPs are the most promising PPs that can be used for the modelling and analysis of cellular networks.

2.4.1   Mathematical Preliminaries

DPPs are the special type of soft-core processes defined on the basis of their n-th order product density functions, $\rho^n : B^n \to [0, \infty)$, where $B^n \subset \mathbb{R}^d$. Consider $\mathbb{C}$ as a complex plane. Let the number $z = z_1 + iz_2$ be a complex number with complex conjugate given by $\bar{z} = z_1 - iz_2$. For a square complex matrix A, let $\det A$ be its determinant. For any function $K : B \times B \to \mathbb{C}$, where $B \subset \mathbb{C}$, let $[K](x_1, \ldots, x_n)$ be the $n \times n$ matrix with $(i, j)'th$ entry $K(x_i, x_j)$. The matrix K is referred to as the *kernel* of the DPP which ensures the existence of particular DPP. In order to guarantee the existence of DPP the

kernel function $K(x, y)$ needs to be continuous, Hermitian, locally square integrable and non-negative [24].

Definition 5. *A PP Φ is said to be a DPP with kernel K if its joint intensities satisfy:*

$$\rho^n(x_1, \cdots, x_k) = det(K(x_i, x_j))_{1 \leq i, j \leq n}, \tag{2.12}$$

for every $n \geq 1$ and $x_1, \cdots, x_n \in \mathbb{C}$.

In particular $\rho = \rho^{(1)}$ is the intensity measure of a DPP, and $g(x, y) = \frac{\rho^{(2)}(x,y)}{\rho(x)\rho(y)}$ is the pair correlation function. The soft-core repulsive nature of the DPPs can be explained by the fact that when two points $x_i \approx x_j$ for $i \neq j$, we have $\rho^{(n)}(x_1, \cdots, x_n) \approx 0$.

2.4.2 Types of DPP

Based on the definition of kernel K following are some of the main types of DPPs as found in literature [22].

1. *Gauss DPP model:* This is defined on the basis of covariance function as

$$K_o(x) = \lambda \exp\left(\frac{-||x||^2}{\alpha^2}\right) \quad x \in \mathbb{R}^2, \tag{2.13}$$

   where λ denotes the intensity and α is the measure of its repulsiveness. The existence of Gauss DPP is ensured by $\lambda \leq (\sqrt{\pi}\alpha)^{-2}$.

2. *Cauchy DPP model:* Covariance function for this model is given by

$$K_0(x) = \frac{\lambda}{(1 + ||x||^2/\alpha^2)^{\nu+1}}, \quad x \in \mathbb{R}^2, \tag{2.14}$$

   where λ is the intensity, α is the scale and ν is the shape parameter. To guarantee the existence of a Cauchy DPP model we require $\lambda \leq \frac{\nu}{(\sqrt{\pi}\alpha)^2}$.

3. *Whittle-Matèrn DPP model:* The covariance function for this process is given as follows:

$$C_0(x) = \rho \frac{2_{1-\nu}}{\Gamma(\nu)} ||x/\alpha||^\nu K_\nu(||x/\alpha||), \quad x \in \mathbb{R}^d, \tag{2.15}$$

   where $K_\nu(.)$ is the modified Bessel function of the second kind with parameter $\nu > 0$, ρ is the intensity, α is the repulsion controlling parameter.

4. *Generalized Gamma DPP model:* This DPP model is defined on the basis of its

spectral intensity as

$$\varphi(x) = \lambda \exp(-||\alpha x||^\nu)\frac{\nu\alpha^2}{2\pi\Gamma(2/\nu)}, \quad x \in \mathbb{R}^2, \tag{2.16}$$

λ is the intensity, α and ν are the scale and shape parameters respectively, and $\Gamma(.)$ denotes the Euler gamma function given as $\Gamma(t) = \int_0^\infty e^{-x}x^{t-1}dx$. The condition on the existence of this DPP model is: $\lambda \leq \frac{2\pi\Gamma(2/\nu)}{\nu\alpha^2}$.

5. *Ginibre DPP model:* The Ginibre point process has the kernel function:

$$K(x,y) = \frac{1}{\pi}e^{-\frac{(|x|^2+|y|^2)}{2}}e^{x\bar{y}}, \quad x,y \in \mathbb{C}, \tag{2.17}$$

with respect to Lebesgue measure on $\mathbb{C}$. Since this PP has been used in this thesis for modelling cellular networks, the following section provides a detailed discussion on this PP.

2.5 β-Ginibre Point Process

The Ginibre point process (GPP), a special type of DPP, was first introduced by J. Ginibre [25] in 1965. Recently this PP has attracted the attention of the wireless research community to model cellular wireless networks because of its repulsion property and analytical tractability.

In this thesis we focus on a more general class of GPP i.e β-GPP $(0 < \beta < 1)$ which is a thinned and rescaled version of a GPP. Formally a β-GPP can be defined as follows:

Definition 6. *The thinned and re-scaled β-GPP is a PP obtained by independently retaining a point in a GPP with probability β and then applying the homothety of ratio* [1] $\frac{1}{\sqrt{\beta}}$ *to maintain the original intensity of the points. The kernel K for β-GPP is given as*

$$K(x,y) = \frac{c}{\pi}e^{-\frac{c\left(|x|^2+|y|^2\right)}{4\beta}}e^{(\frac{c}{\beta})x\bar{y}} \quad x,y \in \mathbb{C}, \tag{2.18}$$

where c is used to control the intensity of the points. In case of 1-GPP $c = 1$.

---

[1]A homothety $H(O,k)$, where O is a fixed point in the plane and k is a nonzero real number, is that transformation that maps point O to itself and maps any other point P to a point $P^{'}$, such that $O, P, P^{'}$ are collinear and $OP^{'} = k.OP$. Point O is called the centre and k is the ratio of homothety.

A special case of interest is, when $\beta \to 0$ the β-GPP converges narrowly to the PPP [26]. The parameter β is used to interpolate smoothly between PPP and 1-GPP. Like the PPP, a β-GPP exhibits unique properties (discussed below) which makes it a very promising PP for modelling cellular networks while maintaining the analytical tractability of the analysis. Below we have mentioned some of the main properties of β-GPP which aid in the analysis of this PP.

- *First-order Density:* Using eq. (2.12) the intensity of a β-GPP can be easily shown to be given by [27]

$$\rho = \frac{c}{\pi}. \tag{2.19}$$

- *Motion Invariance:* Like the PPP, a β-GPP is also motion invariant – translation and rotation does not affect the distribution of the points. This property has also been verified in [27] by showing that the second-order moment density only depends on the distance between the points, given by

$$\rho^2(x, y) = \frac{1 - e^{-|x-y|^2}}{\pi^2} \quad \forall x, y \in \mathbb{C}. \tag{2.20}$$

- *Pair correlation function:* The pair correlation function determines the amount of attraction or repulsion between two points [14]. For a PPP its value is 1 and for a β-GPP it is given by

$$g(x, y) = 1 - e^{(-|x-y|^2)} \quad \forall x, y \in \mathbb{C}. \tag{2.21}$$

It can be seen that $g(x, y) < 1$ which show the repulsive nature of the β-GPP.

- *Distance Distribution:* It is shown in [28] that the squared moduli of the points, in case of β-GPP, in a complex plane are distributed via independent gamma random variables. For a β-GPP the distribution of the distances of the points from the origin is given by [27] as

$$f_{Q_k}(q) = \frac{q^{k-1} e^{-\frac{c}{\beta} q}}{\left(\frac{\beta}{c}\right)^k \Gamma(k)}. \tag{2.22}$$

In Section 2.5.2 we will discuss some more distance distributions for the β-GPP.

2.5.1   Simulation of GPPs

Being easy to simulate is one of the main property of DPPs unlike other repulsive PPs. This section contains a brief exposition on simulating a β-GPP. For more details and discussion about simulating general DPPs readers are requested to see [24] and [29]. Furthermore software developed in [22] is also freely available as a supplement to spatstat [30] for the statistical analysis of DPPs.

As it is shown in eq. (2.22) the squared moduli of distances in β-GPP are distributed via a generalized gamma distribution. However, it should be noted that this does not yield a practical simulation technology since the angles between the points are highly correlated and their distribution is unknown. The idea of simulating a GPP realization was first given by J. Ginibre in his seminal paper [25]. Consider a $N \times N$ hermitian matrix with complex gaussian entries, then the eigenvalues of this matrix are distributed according to the 1-GPP. In order to simulate a β-GPP with a specific value of β, the main idea is to apply independent thinning to the 1-GPP with probability β and then apply the homothety ratio to maintain the original intensity of c/π. Figure 2.3 shows the realization of β-GPP for different values of β. It can be seen easily that when $\beta \to 0$ the realization tends to the realization of PPP. For the case when $\beta = 1$, the points are much more regular, however, there are some points where the points seems to cluster which can be explained via soft-core repulsiveness.

Apart from this, recently [29] and [31] have given sophisticated algorithms for the simulation of β-GPPs. These algorithms are also based on the idea given by [25], so in this work we have used the traditional way of simulating the β-GPP i.e., as given in [25].

2.5.2   Important Distances

One of the main properties of electromagnetic waves is that they attenuate with distance in a wireless medium. It is important that the distribution of the distances between the different points of the process be known. These distances can be used for the performance analysis and comparison of different protocols and algorithms in the wireless network. Here we describe some of the major distances and specialise them for PPPs and β-GPPs.

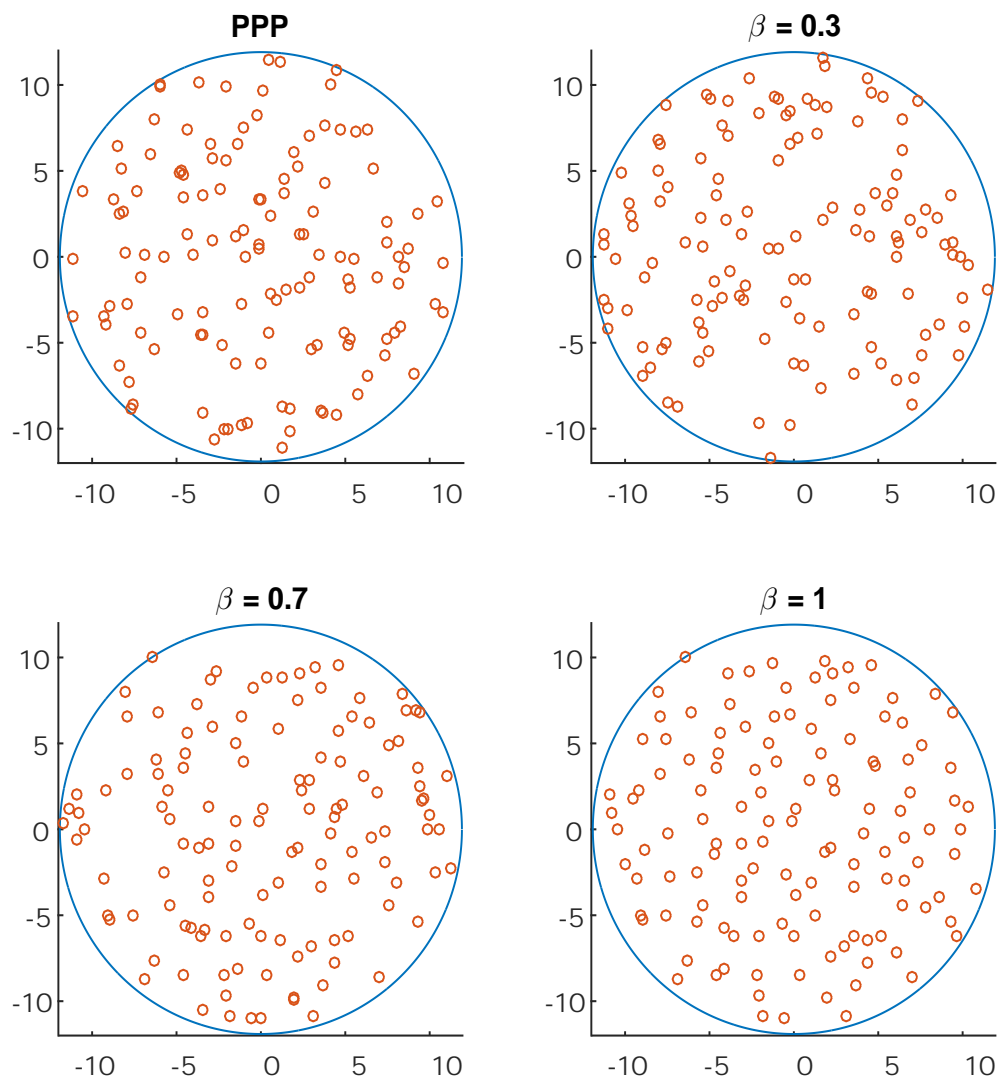1. *Nearest-neighbor distance:* The nearest-neighbor distance is the distance from a

Figure 2.3: Realization of β-GPP with intensity $1/\pi$ for $\beta \to 0$ i.e., PPP, $\beta = 0.3$, $\beta = 0.7$ and $\beta = 1$. In all these cases, the points are distributed in a ball of radius 12 centerd at origin o, i.e., $b(o, 12)$, and $\mathbb{E}[\Phi(b(o, 12)] = 128$.

point $x \in \Phi$ to its nearest neighbor, which is given by $||x - \Phi \backslash \{x\}||$ [14, Def. 2.39] and the corresponding distribution is given by $G^x(r) = \mathbb{P}(||x - \Phi \backslash \{x\}|| \leq r)$.

If Φ is a PPP in $\mathbb{R}^d$ with intensity λ then the distance between a point and its nth neighbour is distributed according to generalized gamma distribution [32, Theorem 1], i.e.,

$$G_n(r) = e^{-\lambda \pi r^2} \frac{2(\lambda \pi r^m)^n}{r \Gamma(n)}. \tag{2.23}$$

In case Φ takes on the realization from the β-GPP then the distance of the first nearest neighbor is given by [27] as

$$G_1(r) = 1 - \prod_{k=2}^{\infty} \left(1 - \beta \tilde{\gamma}\left(k, \frac{c}{\beta} r^2\right)\right), \tag{2.24}$$

where $\tilde{\gamma}(a, x) = (\int_0^{\infty} e_{-u} u^{a-1} \, du)/(\Gamma(a))$ is the normalized incomplete gamma function.

2. *Empty Space Function:* The empty space function or contact distribution function for any PP Φ is the cdf of $||u - \Phi||$ [14, Def. 2.38], and is given by $F_u(r) = \mathbb{P}(||u - \Phi|| \leq r)$.

   If $\Phi \sim \beta$-GPP then from [27] the empty space function is given by

$$F_u(r) = 1 - \prod_{k=1}^{\infty} \left(1 - \beta \tilde{\gamma}\left(k, \frac{c}{\beta} r^2\right)\right). \tag{2.25}$$

   The above equation is proved using the fact that β-GPP is motion-invariant and thus does not depend on u.

3. *The J Function:* The J function is a very useful tool to measure how close a PP is to the PPP, i.e., how much randomness exist in PP. For motion-invariant PPs, it is the ratio of complementary nearest-neighbor distance and contact distribution [14, Def. 2.40]:

$$J(r) = \frac{1 - G(r)}{1 - F(r)} \quad for \ r \geq 0. \tag{2.26}$$

   For a homogeneous PPP, $J(r) = 1$ indicating that it is the complete random process. Values of $J(r) > 1$ indicate repulsion since the chances of having a nearby point are small. On the other hand, $J(r) < 1$ indicates a clustered PP.

If $\Phi \sim \beta$-GPP then the J function using eqs. (2.24) and (2.25) is given by

$$J(r) = \frac{1}{1 - \beta + \beta e^{-(c/\beta)r^2}}. \tag{2.27}$$

In this case the value of $J(r)$ is greater than 1 indicating that β-GPP is a repulsive PP and as $\beta \to 0$ the $J(r)$ becomes equal to 1 i.e., the PPP.

4. *Ripley's K Function:* Using K function, inference about the point pattern can be made about whether the points are randomly distributed, clustered or exhibit repulsion. Ripley [33] defined the K function, also known as reduced second order moment function, for the stationary PP such that $\lambda K(r)$ is the expected number of points y of the process that satisfy $0 < ||x - y|| \leq r$ for a given point x of the process i.e.,

$$\lambda K(r) = \frac{1}{\lambda} \int_{b(x,r)} \rho^2(u) \, du, \tag{2.28}$$

where $b(x, r)$ is the ball of radius r centered at point x, and $u = ||x - y||$.

For the PPP the K function is equal to πr^2. Based on the value of the K function following conclusion can be drawn for a PP:

- $K(r) > \pi r^2 \Rightarrow$ clustering in PP.

- $K(r) < \pi r^2 \Rightarrow$ inhibition among points.

If $\Phi \sim \beta$-GPP then from [27] we have

$$K(r) = \pi r^2 - \frac{\beta \pi}{c} \left(1 - \exp(-\frac{c}{\beta} r^2) \right). \tag{2.29}$$

In this case, since $K(r) < \pi r^2$, the β-GPP exhibits repulsion and is more regular than a PPP. It can be shown easily that when $\beta \to 0$, the above expression results in πr^2, which is the K function for PPP.

So far we have discussed various PPs that can be used for the modelling of cellular networks. Apart from just modelling, we need some tools i.e., *Stochastic Geometry tools* for the analysis of models. The existence of stochastic geometry tools for specific PPs leads to the selection of that particular PP. In the following section we will discuss some important stochastic geometry tools for the analysis of PPs.

2.6 Stochastic Geometry Tools

In many wireless networks the sums and products of functions evaluated at certain point of the PP are of great importance. The most prominent is the computation of aggregate interference, which is the sum of all the interfering signal powers emitted from the random locations in the network. The following two theorems help in evaluating the sum and product for the random locations in the given region.

1. *Campbell's Theorem* [13, Theorem 4.1]: Let Φ be a PP on $\mathbb{R}^d$ and $f : \mathbb{R}^d \mapsto \mathbb{R}$ be a measurable function. Then the expectation of random sum over all the points is given by

$$\mathbb{E}\left(\sum_{x \in \Phi} f(x)\right) = \int_{\mathbb{R}^d} f(x)\lambda(x)\,dx. \tag{2.30}$$

   In the case $\Phi \sim DPP(K)$ then $\lambda(x) = K(x,x)$ i.e., the first order intensity. In case of β-GPP $\lambda(x) = c/\pi$.

2. *Probability Generating Functional (PGFL)* [14, Definition 4.3]: Let Φ be a PP and $\nu(x) : \mathbb{R}^d \mapsto [0,1]$ be a measurable function, then

$$G[v] \triangleq \mathbb{E}\left(\prod_{x \in \Phi} \nu(x)\right) = \mathbb{E}\left[\exp\left(\int_{\mathbb{R}^d} \log \nu(x)\Phi(\,dx)\right)\right]. \tag{2.31}$$

   The PGFL for a PPP with intensity measure Λ is given by [14, Theorem 4.9] as

$$G[v] = \exp\left(-\int_{\mathbb{R}^d} [1 - \nu(x)]\Lambda(\,dx)\right). \tag{2.32}$$

   For $\Phi \sim DPP(K)$ and for measurable function $\nu(x)$, if $\log(\nu)$ satisfies the following three conditions:

   (a) $\lim_{|x|\to\infty} \nu(x) = 0$

   (b) $\lim_{r\to\infty} \int_{\mathbb{R}^2 \setminus B(0,r)} K(x,x)\nu(x)\,dx = 0$

   (c) $\int_{\mathbb{R}^2} K(x,x)(1 - \exp(-\nu(x)))\,dx < +\infty$

then the PGFL is given by [34, Corollary 1]

$$G[v] = \sum_{n=0}^{\infty} \frac{(-1)^n}{n!} \int_{(\mathbb{R}^2)^n} \det(K(x_i, x_j))_{1 \le i,j \le n} \prod_{i=1}^{n} (1 - \nu(x_i)) \, dx_1 \cdots dx_n \quad (2.33)$$

2.6.1 Palm Measures

Palm measures are the counterparts to the conditional distributions in case of PPs, and they are normally used when a PP is conditioned to have a point at $x \in \mathbb{R}^d$. For wireless networks, the Palm distributions are normally used to calculate the outage probability which require having a transmitter/receiver at a specific place. In case the wireless network is modelled via a PPP, Slivnyak's theorem can be used which says that *"adding a point to the origin o does not affect the overall distribution of points"* [14, Theorem 8]. However for DPP, under the reduced Palm distribution, a DPP has the law of another DPP whose kernel is given in closed form by [35, Theorem 1.7], which we have described in the following proposition.

Proposition 1. *Consider* $\Phi \sim DPP(K)$, *where the kernel* K *guarantees the existence of* Φ. *Then under the reduced Palm distribution at* $x_o \in \mathbb{R}^2$ *the kernel* $K_{x_o}^!(x, y)$ *is given by*

$$K_{x_o}^!(x, y) = \frac{1}{K(x_o, x_o)} \det \begin{bmatrix} K(x, y) & K(x, x_o) \\ K(x_o, y) & K(x_o, x_o) \end{bmatrix}. \quad (2.34)$$

2.7 Conclusion

In this chapter we have developed the mathematical base required for the analysis of cellular networks using the recently adopted methodology of stochastic geometry. In particular, we first discussed the PP theory followed by a brief overview of the most popular PPs. In order to capture the underlying separation of BSs in cellular networks, major repulsive PPs like Matérn hard-core process, Gibbs processes and DPPs were also described. Some appealing properties of DPPs, β-GPP in particular, were also discussed to show their analytical tractability. At various levels of explanation limiting cases of

β-GPP where it converges to a PPP, were also discussed in this chapter.

Chapter 3

Load-Aware Modelling in Ginibre Configured Network

3.1 Introduction

Due to the remarkable work of Shannon [36] in the 20th century, Signal-to-Interference-plus-Noise-Ratio (SINR) becomes the most important performance metric for the evaluation of wireless cellular networks. On a given link between the wireless transmitter and receiver, the SINR determines the bit error rate, coverage probability (i.e., SINR exceeds some threshold) and capacity (i.e., maximum achievable rate). Thus, cellular network operators need to know the overall statistics related to SINR (i.e spatial distribution of SINR) in order to optimize the whole network.

The traditional way to determine the spatial distribution of SINR for given link is via the use of extensive simulation [37]. Simulations certainly have the advantage of being able to analyse specific scenarios to any desired depth. However, the major drawback of simulations is that to simulate every possible scenario separately which makes them too much time consuming and cumbersome. The other possible and promising way of analysing the wireless network is to develop the mathematical framework that can be used for the design and optimization of the networks. In this direction, traditional way is to assume the hexagon or circular footprint for the coverage areas and place the BSs at the center. [38] and [39] provide detailed analyses for hexagon and circular coverage footprint respectively. It can be shown easily that these models, even in the most primitive form, are highly intractable and complex. Besides being analytically intractable, these models are becoming invalid because of random placement of BSs in the network.

3.2   Related Work

Recently stochastic geometry tools have gained the attention of wireless research community to model the topological randomness of wireless networks. In this approach, the locations of BSs are taken from random point process [40]. In literature the most widely used model is the PPP to model wireless networks. The history of using PPP for the modelling of cellular networks goes back to 90's [41], in which the authors computed various performance metrics of the cellular networks. After that PPP was mainly used for the modelling of wireless ad hoc networks [42–44]. However, [12] has again captured the attention of research community to use PPP as a modelling tool for cellular networks in 2011. The authors in [12] provided the downlink coverage model for a single-tier cellular network with PPP configured BSs. At the same time, the authors in this work compared the performance of PPP and grid based models with actually deployed BS configuration and found that the PPP is the most pessimist in terms of coverage and mean transmission rate analysis whereas quite the opposite with grid-based models. The major drawback of using PPP is that this model assume the independent placement of points in a given region which is not the case in cellular network, since the locations of BSs are negatively correlated.

In order to capture the underlying separation between BSs a new class of repulsive PPs, i.e., DPPs, have been recently proposed which are much more analytical tractable and at the same time accurate. In [45], the GPP is proposed to model the cellular networks. The authors in this work computed the coverage probability for a single tier cellular networks and showed that the GPP is more accurate as compared to PPP. Similarly, [27] used the more general class of GPP i.e., β-GPP to control the repulsion between the BSs in a single tier cellular network by tunning the parameter β. Several statistical parameters were also provided in this work for β-GPP configured network. The downlink coverage analysis under Nakagami-m fading channel is provided in [46] with GPP configured BSs. Recently an effort has been made in [34] to convince the research community to use the DPP for the modelling of cellular networks, where various statistical parameters like empty space function, nearest neighbour function, mean interference and downlink SIR distribution were analysed. The authors in this work used three models of DPPs, namely Gauss, Cauchy and Generalized Gamma DPP, and found that they best fit the actual

deployment scenario in terms of the coverage probability and at the same time were much more tractable.

Despite the encouraging progress, these models lack in at least one most important aspect i.e., neglect of network traffic load. Almost all the previous work [27, 34, 45, 46] assumed that all the BSs in the network are transmitting at all the times, which translates into full load scenario resulting in pessimistic estimates of coverage analysis. The main goal of this chapter is to use the more realistic model for the location of BSs in the network while introducing the idea of BS load for coverage analysis. Here we use the idea of conditional thinning of interference field, as given by [47] for PPP case, to model the BS load.

3.3 System Model

Consider a single tier cellular network in which the BSs are randomly distributed in the specific region. The locations of BSs are represented by the set $\Phi = \{x_i\}$, $i \in \mathbb{N}$, where the order $x_1, x_2, \cdots$ is arbitrary. We assume, the set Φ takes on the realization of the GPP, where $x_i's$ are the points of the process. Further, we assume that the set $\zeta = \{U_i\}$, $i \in \mathbb{N}$, represents the location of the mobile users. These mobile users are uniformly distributed and can be modelled by the homogeneous independent PPP with intensity λ_M. Each mobile user is connected to its nearest BS, that is, the mobile users in the voronoi cell of the BS are associated with that station. We perform all the analysis on the typical user located at the origin, which is permissible due to Slivnyak's theorem [14] for homogeneous PPPs and due to the motion invariance property of GPPs.

We assume the standard power loss model with path loss exponent $\alpha > 2$ and each BS is transmitting with constant power P. In order to model random wireless channel effects, we assume that mobile users experience only Rayleigh fading with mean 1, which we denote by $h \sim \exp(1)$. Under these assumptions the received power at a typical user, connected to BS located at point x_o, is given by $P_r = P h_{x_o} |x_o|^{-\alpha}$. The interference power at a typical receiver is the sum of the received powers from all the BSs except the home BS, i.e $I_r = P \sum_{x_i \in \Phi/x_o} h_{x_i} |x_i|^{-\alpha}$. The noise power σ^2, is assumed to be additive and is assumed negligible compared to the interference. Under these assumptions the expression

of SINR is given by

$$\text{SINR} = \frac{Ph_{x_o}|x_o|^{-\alpha}}{P\sum_{x_i \in \Phi/x_o} h_{x_i}|x_i|^{-\alpha} + \sigma^2}. \tag{3.1}$$

For some SINR coverage threshold T, the coverage probability is given by

$$\text{P}_c = \mathbb{P}(\text{SINR} > T/ |x_o| \leq |x_i|) \ \forall i \in \mathbb{N}. \tag{3.2}$$

For analytical tractability purposes, we assume the value of the coverage threshold T to be greater than 1 (0 dB), i.e., $T > 1$. Under this assumption at most one BS in the whole network can connect to the typical user. This assumption seems to be dubious, but this can be justified by the fact that we are focusing on the user located in the middle of the cell. In actual scenario, only users at cell edges have operating SIR less than 0 dB because of the interference. In order to facilitate the edge users more sophisticated interference mitigation techniques like coordinated multipoint (CoMP) [48] are under the process of investigation, which does not come under the scope of this work. This assumption has already been used in literature [8], [47] for the PPP model. For detailed discussion on this assumption see [8, Lemma 1].

3.4   Conditional Laplace Transform of Interference

If the desired signal power in the wireless network is exponentially distributed, such as Rayleigh fading, the coverage probability is given by the Laplace transform of the interference measured at the receiver [14, Box 5.1]. For the case when the wireless transmitters are distributed via PPP the Laplace transform of interference has already been computed in [12] for single tier cellular networks and in [8] for multi-tier cellular networks. In this section we derive an upper bound on the expression of the Laplace transform of interference when the BSs are distributed according to a β-GPP.

The authors in [34] have given the following expression of the Laplace transform of interference for general motion invariant DPPs under the nearest BS association scheme.

$$\mathbb{E}_{x_o}^![e^{-sI}] = \frac{\sum_{n=0}^{\infty} \frac{(-1)^n}{n!} \int_{(\mathbb{R}^2)^n} \det[K_{x_o}^!(x_i, x_j)_{(1 \leq i,j \leq n)}] \prod_{i=1}^{n}[1 - \frac{\mathbb{1}_{|x_i| \geq |x_o|}}{1 + sPl(x_i)}] \, dx_1 \cdots dx_n}{\sum_{n=0}^{\infty} \frac{(-1)^n}{n!} \int_{B(o,x_o)^n} \det[K_{x_o}^!(x_i, x_j)]_{(1 \leq i,j \leq n)} \, dx_1 \cdots dx_n}, \tag{3.3}$$

where $K_{x_o}^!(x_i, x_j)_{(1 \leq i,j \leq n)})$ is given by eq. (2.34). Since the above equation involves a multiple integration over $\mathbb{R}^2$ we use the diagonal approximation [49] of the matrix determinant

to get the upper bound on the above expression. Specifically, the determinant of the matrix $K^!_{x_o}(x_i, x_j)_{(1 \leq i,j \leq n)}$ is approximated as $\det[K^!_{x_o}(x_i, x_j)]_{(1 \leq i,j \leq n)} \leq \prod_{i=1}^n K^!_{x_o}(x_i, x_i)$. The relative error bound for the diagonal approximation is provided in [49, Theorem 1]. The authors in [34] used this approximation for the coverage probability and showed that it is accurate for high SIR thresholds. In our case, since we are assuming the SIR threshold greater than 0 dB, so this approximation is justified.

Lemma 1. *Consider $\Phi \sim DDP(K)$, where the kernel K ensures the existence of a DPP, then under the reduced Palm measure, the Laplace transform of Interference, under the maximum SIR connectivity scheme and using the diagonal approximation, is given by*

$$\mathcal{L}_I(s)_{x_o} = \exp\left(-\int_{B^c(o,x_o)} K^!_{x_o}(x,x)\left(1 - \frac{1}{1+sPl(x)}\right)dx\right), \qquad (3.4)$$

where $K^!_{x_o}(x,x)$ is the reduced kernel at point x_o given by eq. (2.34), $l(x)$ is the distance based path loss given by $|x|^{-\alpha}$, where $|.|$ is the Euclidean distance and α is the path loss exponent.

Proof. From [34, Theorem 1], the expression for the Laplace transform of interference for a general DPP is given by

$$\mathbb{E}^!_{x_o}[e^{-sI}] = \frac{\sum_{n=0}^{\infty} \frac{(-1)^n}{n!} \int_{(\mathbb{R}^2)^n} \det[K^!_{x_o}(x_i, x_j)]_{(1 \leq i,j \leq n)} \prod_{i=1}^n [1 - \frac{\mathbb{1}_{|x_i| \geq |x_o|}}{1+sPl(x_i)}] dx_1 \cdots dx_n}{\sum_{n=0}^{\infty} \frac{(-1)^n}{n!} \int_{B(o,x_o)^n} \det[K^!_{x_o}(x_i, x_j)]_{(1 \leq i,j \leq n)} dx_1 \cdots dx_n}. \tag{3.5}$$

Using the diagonal approximation the above upper bound on the above expression is given by:

$$\mathbb{E}^!_{x_o}[e^{-sI}] \leq \frac{\sum_{n=0}^{\infty} \frac{(-1)^n}{n!} \int_{(\mathbb{R}^2)^n} \prod_{i=1}^n (K^!_{x_o}(x_i, x_i)[1 - \frac{\mathbb{1}_{|x_i| \geq |r_o|}}{1+sPl(x_i)}]) dx_1 \cdots dx_n}{\sum_{n=0}^{\infty} \frac{(-1)^n}{n!} \int_{B(o,x_o)^n} \prod_{j=1}^n K^!_{x_o}(x_j, x_j) dx_1 \cdots dx_n}. \tag{3.6}$$

It can be observed from the above equation that it involves the Taylor series expansion of $\exp(-x)$, i.e., $\sum_{n=0}^{\infty} \frac{(-1)^n}{n!} x^n = \exp^{-x}$. Thus we obtain

$$\mathbb{E}^!_{x_o}[e^{-sI}] \leq \frac{\exp\left(-\int_{\mathbb{R}^2} K^!_{x_o}(x,x)(1 - \frac{\mathbb{1}_{|x| \geq |x_o|}}{1+sPl(x)}) dx\right)}{\exp(-\int_{B(o,x_o)} K^!_{x_o}(x,x) dx)}. \tag{3.7}$$

Due to the indicator function $\mathbb{1}_{|x_i| \geq |x_o|}$ being in the integrand in the numerator, the above

expression can be divided in two parts as follows:

$$\mathbb{E}^!_{x_o}[e^{-sI}] \leq \frac{\exp\left(-\int_{B(o,x_o)} K^!_{x_o}(x,x)\,dx - \int_{B^c(0,x_o)} K^!_{x_o}(x,x)\left(1 - \frac{1}{1+sPl(x)}\right)dx\right)}{\exp\left(-\int_{B(o,x_o)} K^!_{x_o}(x,x)\,dx\right)} \tag{3.8}$$

$$= \exp\left(-\int_{B^c(o,x_o)} K^!_{x_o}(x,x)\left(1 - \frac{1}{1+sPl(x)}\right)dx\right), \tag{3.9}$$

where the latter expression involves simply the cancellation of the same integral in the numerator and denominator, which completes the proof. $\qquad\square$

As discussed before, the aggregate interference is the sum of powers from all the transmitters except the intended one. In the case of a PPP removing one point from the overall distribution is simple due to Slivnyak's theorem. However, in the case of DPPs removing one point from the overall realization of points alters the kernel of DPP. Fortunately, the expression for the kernel under reduced Palm measure is known and given by eq. (2.34). In the following Lemma we have provided the reduced kernel for a β-GPP

Lemma 2. *Consider $\phi \sim \beta$-GPP(K), where the kernel K is given by eq. (2.18). Then under the reduced Palm distribution at $x_o \in \mathbb{R}^2$ the kernel $K^!_{x_o}(x,y)$ is given by*

$$K^!_{x_o}(x,y) = \frac{c}{\pi} e^{-\frac{c}{\beta}(x^2+y^2)}\left(e^{\frac{c}{\beta}x\overline{y}} - e^{-\frac{c}{\beta}x_o^2}e^{\frac{c}{\beta}(x\overline{x}_o + x_o\overline{y})}\right). \tag{3.10}$$

The above Lemma can easily be proved by putting the β-GPP kernel (eq. (2.18)) in eq. (2.34). The intensity of the points under the reduced Palm distribution of β-GPP is given by

$$K^!_{x_o}(x,x) = \frac{c}{\pi}\left(1 - e^{-\frac{c}{\beta}(|x-x_o|^2)}\right) \tag{3.11}$$

In the following theorem we specialize eq. (3.4) to the case of a β-GPP model.

Theorem 1. *Consider $\Phi \sim \beta$-GPP(K) where the kernel K is given by eq. (2.18) and the intended BS is located at point x_o then the Laplace transform of interference is given by*

$$\mathcal{L}_I(s)_{x_o} = \exp\left(-\frac{2csP}{\alpha}E_1(sP + r_o^\alpha) - \beta\pi\left(\frac{\pi}{2} - \sqrt{\frac{\beta}{c}}e^{-\frac{4r_o^2 c}{\beta}}\gamma\left(\frac{1}{2}, \frac{4r_o^2 c}{\beta}\right)\right) + \mathcal{X}(s,\alpha,\beta)\right), \tag{3.12}$$

where $\mathcal{X}(s,\alpha,\beta) = 2\pi\left(\int_{r_o}^{\infty} \frac{e^{-\frac{c}{\beta}(r-r_o)^2}}{1+sPr^{-\alpha}}\,dr\right)$ and $E_1(z) = \int_0^{\infty} e^{-zt}t^{-1}dt$. The above expression can easily be derived for the case of a 1-GPP by putting the value of β and c equal

to 1.

Proof. Equation 3.4 can be specialized for the case of a β-GPP by putting eq. (3.11) in eq. (3.4), and the result is as follows

$$\mathbb{E}^!_{x_o}[e^{-sI}] = \exp\left(-\frac{c}{\pi}\int_{B^c(o,x_o)}\left(\frac{sP|x|^{-\alpha}}{1+sP|x|^{-\alpha}} + \frac{e^{-\frac{c}{\beta}|x-r_o|^2}}{1+sP|x|^{-\alpha}} - e^{-\frac{c}{\beta}|x-x_o|^2}\right)dx\right) \quad (3.13)$$

$$= \exp\left(-\frac{c}{\pi}(A_1 + A_2 - A_3)\right). \quad (3.14)$$

Since the above integral involves a long equation we have split the integral and below we provide the solutions of the individual integrals.

Solution of A_1: After converting from Cartesian to polar coordinates and using $|x| = r$, the integral A_1 can be written as

$$\int_{B^c(o,x_o)} A_1\, dx = \int_{B^c(0,x_o)}\frac{sP|x|^{-\alpha}}{1+sP|x|^{-\alpha}}\, dx = \int_0^{2\pi}\int_{r_o}^{\infty}\frac{sP}{sP+r^\alpha}r\, dr\, d\theta. \quad (3.15)$$

Using the substitution $r^2 \leftarrow u$ we have the following (note the integration limit will now change to r_o^2 to ∞).

$$A_1 = \pi\int_{r_o^2}^{\infty}\frac{sP}{sP+u^{\alpha/2}}\, du. \quad (3.16)$$

In order to simplify it further we use the fact that $\int_0^{\infty}e^{-at}dt = 1/a$ and write the above equation as

$$A_1 = \pi sP\int_{r_o^2}^{\infty}\int_{t=0}^{\infty}e^{-t(sP+u^{\alpha/2})}\, dt\, du. \quad (3.17)$$

Here we can change the order of integration and after simplifying with respect to u we have

$$A_1 = \frac{2\pi sP}{\alpha}\int_{t=0}^{\infty}e^{-t(sP+r_o^\alpha)}t^{-1}\, dt. \quad (3.18)$$

From [50] we know that $\int_0^{\infty}e^{-zt}t^{-1}dt = E_1(z)$ for $Re\{z\} > 0$ and the final result can be written as

$$A_1 = \frac{2\pi sP}{\alpha}E_1(sP+r_o^\alpha). \quad (3.19)$$

Solution of A_2: The solution of the second integral is straight forward and can be obtained by simply converting from Cartesian to polar coordinates

$$\int_{B^c(o,x_o)} A_2\, dx = 2\pi\left(\int_{r_o}^{\infty}\frac{e^{-\frac{c}{\beta}(r-r_o)^2}}{1+sPr^{-\alpha}}\, dr\right). \quad (3.20)$$
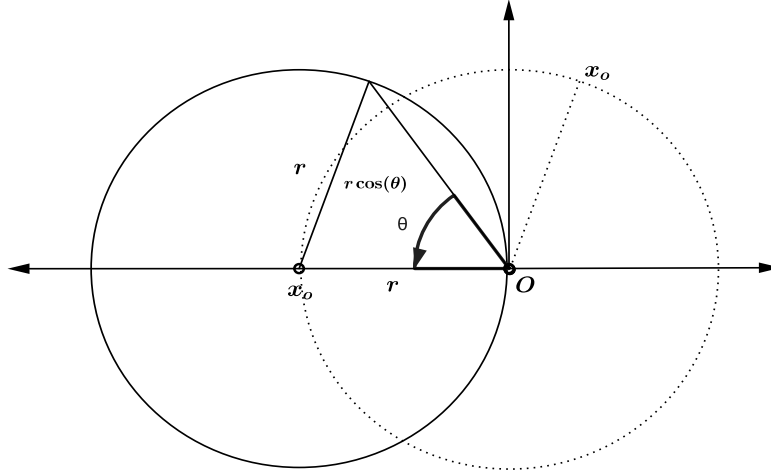
Figure 3.1: The effect of transformation, $u \leftarrow |x - x_o|$, on the integral A_3. The dashed circle represent the placement of ball before transformation and solid circle represent after transformation. The triangle is used to find the limits of integration after transformation.

Solution of A_3: The third integral of eq. 3.13 is given by

$$A_3 = \int_{B^c(o,x_o)} e^{-\frac{c}{\beta}|x-x_o|^2} dx. \tag{3.21}$$

The above integral needs to be integrated on the whole plane i.e., $\mathbb{R}^2$ except the ball of radius $|x_o|$ centred at origin o. The simplest way of doing so is to integrate it on the whole plane and then subtract the area of ball from the result which can be written as follows

$$\int_{B^c(o,x_o)} e^{-\frac{c}{\beta}|x-x_o|^2} dx = \int_{\mathbb{R}^2} e^{-\frac{c}{\beta}|x-x_o|^2} dx - \int_{B(o,x_o)} e^{-\frac{c}{\beta}|x-x_o|^2} dx. \tag{3.22}$$

Now converting from Cartesian to polar coordinates and using transformation $u \leftarrow |x-x_o|$ we get

$$\int_{B^c(o,x_o)} e^{-\frac{c}{\beta}|x-x_o|^2} dx = \int_0^{2\pi} \int_0^{\infty} e^{-\frac{c}{\beta}u^2} u\, du\, d\theta - 2\int_0^{\pi/2} \int_0^{2r_o cos(\theta)} e^{-\frac{c}{\beta}u^2} u\, du\, d\theta. \tag{3.23}$$

The first integral in the above equation is straight forward and can be easily computed by substituting $u^2 \leftarrow x$. The limits in the second integral can be well explained using

Figure 3.1, where we have used the law of cosine to obtain the upper limit as $r_o \cos(\theta)$. Further, using the fact that $\int_{\theta=0}^{\frac{\pi}{2}} \int_{r=0}^{2r_o \cos(\theta)} f(r, \theta) \, du \, d\theta = \int_{r=0}^{r_o} dr \int_{\theta=0}^{\arccos(r/2r_o)} f(r, \theta) \, d\theta$ [50, eq. 4.614, p. 617], and integrating with respect to θ we get the following result

$$A_3 = \int_{B^c(0,r_o)} e^{-\frac{c}{\beta}|x-r_o|^2} \, dx = \frac{\pi\beta}{c} - 2 \int_0^{2r_o} e^{-\frac{c}{\beta}u^2} \arccos\left(\frac{u}{2r_o}\right) u \, du. \tag{3.24}$$

Using the substitution $u^2 \leftarrow x$ we get the following results

$$A_3 = \frac{\pi\beta}{c} - \frac{\beta\pi}{2c} - \frac{\beta}{c} \int_0^{4r_o^2} \frac{e^{-\frac{c}{\beta}x}}{\sqrt{4r_o^2 - x}} \, dx \tag{3.25}$$

$$A_3 = \frac{\beta}{c}\left(\frac{\pi}{2} - \sqrt{\frac{\beta}{c}} e^{-\frac{4r_o^2 c}{\beta}} \gamma\left(\frac{1}{2}, \frac{4r_o^2 c}{\beta}\right)\right), \tag{3.26}$$

where the final result is obtained by using $\int_0^u (u-x)^\nu e^{-\mu x} \, dx = \mu^{-\nu-1} e^{-u\mu} \gamma(\nu+1, -u\mu)$ $\{Re\,\nu > -1, u > 0\}$ [50, eq. 3.382(1), p. 318], where $\gamma(a, b)$ is the incomplete gamma function given by $\gamma(a, b) = \int_0^b e^{-t} t^{a-1} dt$. Combining the results of A_1, A_2 and A_3 in eq. (3.13) we get the final result. □

According to [26, Theorem 4], the Laplace functional of a β-GPP converges narrowly to that of a PPP with intensity $K(x, x)$. In the following corollary we verify this result in our case

Corollary 1. *Since a PPP is the limit of a β-GPP when $\beta \to 0$, setting $\beta \to 0$ in eq. 3.13 the Laplace transform of interference in case of PPP with intensity $\frac{c}{\pi}$ is given by*

$$\mathcal{L}_I(s)_{r_o} = \exp\left(-\frac{2csP}{\alpha} E_1(sP + r_o^\alpha)\right) \tag{3.27}$$

which is consistent with eq. (12) in [12] for $c = 1$.

Proof. This corollary can easily be verified by putting $\lim_{\beta \to 0}$ in eq. (3.12) □

3.4.1 Modelling BS Load

As mentioned in the system model, we assume that a typical user connects to the strongest BS in terms of received SIR. In the case of single tier cellular networks, the nearest BS provides the highest received SIR for each user in the network [34]. We partition whole set of BSs, i.e., Φ in two different sets independently, which are called as Ψ and

Δ, with probabilities β[1] and $1 - \beta$, where Ψ is the set of active BSs and Δ is the set of inactive BSs in a specific time slot. This partition can also be seen as the activity factor of BS, i.e., a specific BS in the whole network is active with probability β in a specific time slot. After this partition, the interferers are now confined to the set Ψ. Since the partition of Φ is done independently, there is a possibility that Δ also contain the serving BS, i.e., the closest one. This BS load model is proposed by Dhillon *et al* in [47] in the case when the BSs are distributed according to a PPP. We define the maximum signal strength from the set of nodes $\mathcal{K}$ as

$$M(\mathcal{K}) = \sup_{x \in \mathcal{K}} P h_x |x|^{-\alpha} \mathbb{1}_{\{x \in \mathcal{K}\}}. \tag{3.28}$$

Since, after partition, we have two sets of nodes, i.e., Ψ and Δ the $\mathbb{E}[\mathbb{1}_{x \in \mathcal{K}}]$ represent the probability that x belong to a particular set. The total received power is given as

$$I = \sum_{x \in \Phi} P h_x |x|^{-\alpha} \mathbb{1}_{\{x \in \Psi\}}. \tag{3.29}$$

Here $\mathbb{1}_{\{x \in \Psi\}}$ denotes the indicator function for the active BSs, and $\mathbb{E}[\mathbb{1}_{x \in \Psi}] = \beta$. The total received power in the above expression also contains the power from the serving BS if a typical user is connected to an active BS.

3.5 Coverage Probability for Active BSs

In this section we provide the expression of coverage probability for active BSs (Ψ) only, neglecting the fact that serving BS may lie in idle set (Δ). Later we will show that how this expression is used for the load-aware scenario. The Laplace transform of interference can be used to find the coverage probability for the active BS sets. The expression of coverage probability has already been provided in [27] for a single-tier and in [51] for multi-tier β-GPP configurated network. In [45] authors provide the coverage probability expression for 1-GPP cellular network model. The authors in the same work also provide the coverage probability expression for frequency reuse scenario by independently assigning the frequency band to each set of BSs. Although the expression of coverage probability can be used directly from [45] in our analysis, we go through the derivation of the following

---

[1]This β can be seen as the probability of retaining points in GPP to get Ψ.

expression in order to assist the reader in understanding the proof of GPP for load aware scenario.

Proposition 2. *Consider a single tier cellular network model and after applying independent thinning with probability β the coverage probability for the set of remaining active BSs is given as*

$$\mathbb{P}(\mathsf{SIR} > T) = \int_0^\infty e^{-v} F(v, T, \alpha, \beta) G(v, T, \alpha, \beta) dv, \tag{3.30}$$

where

$$F(v, T, \alpha, \beta) = \prod_{j=1}^\infty \frac{1}{(j-1)!} \int_v^\infty s^{j-1} e^{-s} \left[1 - \beta \left[1 - \left(1 + T \left(\frac{v}{s} \right)^{\alpha/2} \right)^{-1} \right] \right] ds, \tag{3.31}$$

$$G(v, T, \alpha, \beta) = \sum_{i=1}^\infty v^{i-1} \left(\int_v^\infty s^{i-1} e^{-s} \left[1 - \beta \left[1 - \left(1 + T \left(\frac{v}{s} \right)^{\alpha/2} \right)^{-1} \right] \right] ds \right)^{-1}. \tag{3.32}$$

Proof. Using the definition of SINR as given in eq. (3.1), neglecting noise (σ^2), the expression of coverage probability is given as

$$\mathbb{P}_c = \sum_{i=1}^\infty \mathbb{P} \left(\frac{P h_{x_i} |x_i|^{-\alpha}}{\sum_{j \in \mathbb{N} \setminus i} P h_{x_j} |x_j|^{-\alpha}} > T, |x_i| \leq |x_j|, x_. \in \Psi \right) \quad j \in \mathbb{N}. \tag{3.33}$$

Since h_{x_i} is exponentially distributed with mean 1, i.e., $h \sim \exp(1)$ and power P is constant for all the BSs, we have

$$\mathbb{P}_c = \sum_{i=1}^\infty \mathbb{P} \left(h_{x_i} > \frac{T \sum_{j \in \mathbb{N} \setminus i} h_{x_j} |x_j|^{-\alpha}}{|x_i|^{-\alpha}}, |x_i| \leq |x_j|, x_. \in \Psi \right) \quad j \in \mathbb{N} \tag{3.34}$$

$$= \sum_{i=1}^\infty \mathbb{E} \left(\exp \left(-\frac{T \sum_{j \in \mathbb{N} \setminus i} h_{x_j} |x_j|^{-\alpha}}{|x_i|^{-\alpha}} \right) \mathbb{1}_{\{|x_i| \leq |x_j|, x_{(.)} \in \Psi\}} \right) \quad j \in \mathbb{N}. \tag{3.35}$$

Since the partitioning of Φ is done independently with probability β and $1 - \beta$ in two sets which are Ψ and Δ respectively. Hence, $\mathbb{E}[\mathbb{1}(x \in \Psi)] = \beta$. The above equation can now be written as

$$= \sum_{i=1}^\infty \mathbb{E}_{x,h} \left(\exp \left(-\frac{T \sum_{j \in \mathbb{N} \setminus i} h_{x_j} |x_j|^{-\alpha}}{|x_i|^{-\alpha}} \right) \beta + (1 - \beta) \mathbb{1}_{\{|x_i| \leq |x_j|\}} \right). \tag{3.36}$$

Furthermore, $h'_{x_j}s$ are independent of the location of points and are exponentially distributed. Under the condition that $|x_i| \leq |x_j|$ above equation can now further be simplified as

$$= \sum_{i=1}^{\infty} \mathbb{E}_x \left\{ \prod_{j \in \mathbb{N} \setminus i} \left[\left(\frac{1}{1 + T \left(|x_j|/|x_i| \right)^{-\alpha}} \right) \beta + (1 - \beta) \right] \right\}. \qquad (3.37)$$

As mentioned in Chapter 2, eq. (2.22) that the *squared moduli* of the points in a GPP are distributed via generalized gamma distribution. Substituting $(|x_j|)^{-\alpha} = v^{-\alpha/2}$, $(|x_i|)^{-\alpha} = u^{-\alpha/2}$, and conditioning on $|x_i| \leq |x_j|$ the expectation in above equation can further be solved as

$$= \sum_{i=1}^{\infty} \int_0^{\infty} \frac{u^{i-1} e^{-u}}{\Gamma(i)} \left(\prod_{j \in \mathbb{N} \setminus i} \int_u^{\infty} \left[\left(\frac{1}{1 + T \left(\frac{u}{v} \right)^{\frac{\alpha}{2}}} \right) \beta + 1 - \beta \right] \frac{v^{j-1} e^{-v}}{\Gamma(j)} dv \right) du. \qquad (3.38)$$

Note that the limits of inner integral are from u to ∞, this is because of the condition that $|x_i| \leq |x_j|$. Further using $\Gamma(i) = (i-1)!$ and simple arrangement of terms final result is obtained. $\qquad \square$

3.6   Coverage Probability for Load-Aware Scenario

This is the main analytical portion of thesis where we derive an expression for the probability that a typical mobile user is in coverage if all the BSs in the whole network are not transmitting. In this section we incorporate the notion of BS load into the system model developed in Section 3.3.

Using the definition of I and $M(\mathcal{K})$, the coverage probability for these settings can be defined as

Definition 7. *The coverage probability,* P_c *can be formally defined as*

$$\mathsf{P}_c = 1 - \mathbb{E} \left[\mathbb{1} \left(\frac{M(\Psi)}{I - M(\Psi)} < T \right) \mathbb{1} \left(\frac{M(\Delta)}{I} < T \right) \right] \qquad (3.39)$$

This definition involves the computation of the probability of outage which leads to the coverage probability i.e., $\mathbf{P}_c = 1 - \mathsf{P}_o$. The first indicator function in the expectation represents the event when the mobile user is connected to an active BS in which case the interference power is given as $I - M(\Psi)$. It can be seen easily from the above definition that $\mathbb{1} \left(\frac{M(\Psi)}{I - M(\Psi)} < T \right) = 1$ if no BS in the active set is able to connect to the mobile user.

The second indicator function covers the fact that a serving BS may lie in the set Δ in which case the total received power given by eq. (3.29) will act as an interference power. In this case $\mathbb{1}\left(\frac{M(\Delta)}{I} < T\right) = 1$ only if no BS in the idle set is able to provide the desired SIR to the mobile user. So a mobile user is considered to be in outage if no BS (from both of the sets) in the network provides the required SIR.

If all the BSs in the whole network transmit with the probability 1 then $\#(\Phi) = \#(\Psi)^2$ and $\#(\Delta) = 0$, and the above definition of P_c reverts to full load scenario. In following theorem we provide the expression for the coverage probability for load aware scenario

Theorem 2. *Consider a GPP configured single tier cellular network in which the BSs are transmitting with the probability β, then the downlink coverage probability for a typical user assuming coverage threshold $T > 1$, is*

$$\mathsf{P}_c = \int_0^\infty e^{-v} F(v, T, \alpha, \beta) G(v, T, \alpha, \beta) dv - \sum_{m=1}^\infty \frac{(-A)^m}{m!} \int_0^\infty C(s, m)\, ds, \qquad (3.40)$$

where

$$F(v, T, \alpha, \beta) = \prod_{j=1}^\infty \frac{1}{(j-1)!} \int_v^\infty s^{j-1} e^{-s} \left[1 - \beta \left[1 - \left(1 + T \left(\frac{v}{s}\right)^{\alpha/2}\right)^{-1}\right]\right] ds, \qquad (3.41)$$

$$G(v, T, \alpha, \beta) = \sum_{i=1}^\infty v^{i-1} \left(\int_v^\infty s^{i-1} e^{-s} \left[1 - \beta \left[1 - \left(1 + T \left(\frac{v}{s}\right)^{\alpha/2}\right)^{-1}\right]\right] ds\right)^{-1}, \qquad (3.42)$$

$$C(s, m) = \mathcal{L}_I(s) - K(x, x) \int_{\mathbb{R}^2} \frac{\mathcal{L}_I\left(s + TP^{-1}|x|^\alpha\right)}{1 + sP|x|^{-\alpha}} dx, \qquad (3.43)$$

$$A = T^{-\frac{2}{\alpha}} P^{\frac{2}{\alpha}} (1 - \beta)^{\frac{2}{\alpha}} \Gamma\left(1 + \frac{2}{\alpha}\right). \qquad (3.44)$$

Proof. The coverage probability is given by eq. (3.39). Since the set Δ and corresponding fading random variables are independent, we can move the expectation inside while conditioning on the common interference. Hence

$$1 - \mathsf{P}_c = \mathbb{E}\left[\mathbb{1}\left(\frac{M(\Psi)}{I - M(\Psi)} < T\right) \mathbb{E}_{\Delta,h}\left(\mathbb{1}\left(M(\Delta) < TI\right)\right)\right]. \qquad (3.45)$$

$^2\#(.)$ denotes the number of elements in the set (.).

We first simplify the second expectation, which can be written as follows:

$$\mathbb{E}_{\Delta,h}\left(\mathbb{1}\left(M(\Delta) < TI\right)\right) \tag{3.46}$$

$$= \mathbb{E}_{\Delta,h}\left(\prod_{x\in\Delta} \mathbb{1}\left(Ph_x|x|^{-\alpha}\mathbb{1}_{\{x\in\Delta\}} < TI\right)\right) \tag{3.47}$$

$$= \mathbb{E}_{\Delta,h}\left(\prod_{x\in\Delta} \mathbb{1}\left((Ph_x|x|^{-\alpha})(1-\beta) < TI\right)\right) \tag{3.48}$$

$$= \mathbb{E}_{\Delta,h}\left(\prod_{x\in\Delta}\left[h_x < \frac{TI}{(P|x|^{-\alpha})(1-\beta)}\right]\right) \tag{3.49}$$

$$= \mathbb{E}_{\Delta}\left(\prod_{x\in\Delta}\left[1 - \exp\left(-\frac{(TI)|x|^{\alpha}}{P(1-\beta)}\right)\right]\right). \tag{3.50}$$

Here it can be seen that by putting $\beta = 1$, i.e., all the BSs in the network are transmitting then the above eq. results in $\mathbb{E}\left(\prod_{x\in\Delta}(1)\right) = 1$. Now using eq. (2.33), i.e., PGFL for DPP, and applying it to above equation we have

$$= \sum_{n=0}^{\infty} \frac{(-1)^n}{n!} \int_{(\mathbb{R}^2)^n} \det(K(x_i, x_j))_{1\leq i,j\leq n} \prod_{i=1}^{n}\left[\left(\exp\left(-\frac{(TI)|x_i|^{\alpha}}{P(1-\beta)}\right)\right)\right] dx_i \cdots dx_n. \tag{3.51}$$

Since eq. (3.51) involves multiple integration over $\mathbb{R}^2$, we use the diagonal approximation to simplify it further which can be written in exponential form as

$$= \exp\left(-\frac{1}{\pi}\int_{\mathbb{R}^2} \exp\left(-\frac{(TI)|x|^{\alpha}}{P(1-\beta)}\right) dx\right). \tag{3.52}$$

After converting from Cartesian to polar coordinates an integrating with respect to θ we have

$$= \exp\left[-\frac{2\pi}{\pi}\int_0^{\infty} \exp\left(-\frac{TI}{P(1-\beta)}r^{\alpha}\right) r\,dr\right]. \tag{3.53}$$

Using transformation $u \leftarrow r^{\alpha}$

$$= \exp\left[-2\int_0^{\infty} \exp\left(-\frac{TI}{P(1-\beta)}u\right)\frac{1}{\alpha}u^{2/\alpha-1}du\right]. \tag{3.54}$$

Now again using transformation $v \leftarrow \frac{TI}{P(1-\beta)}u$, note that integration limit do not change

$$= \exp\left[-\frac{2}{\alpha}\left(\frac{TI}{P(1-\beta)}\right)^{-2/\alpha}\int_0^{\infty} \exp(-v)v^{2/\alpha-1}dv\right]. \tag{3.55}$$

Since $\int_0^\infty e^{-x} x^{t-1} = \Gamma(t)$ above equation can now be written as

$$= \exp\left[-\frac{2}{\alpha}\left(\frac{TI}{P(1-\beta)}\right)^{-2/\alpha}\Gamma\left(\frac{2}{\alpha}\right)\right]. \tag{3.56}$$

Using the fact that $\Gamma(1+t) = t\Gamma(t)$ we have

$$= \exp\left[-\frac{T^{-\frac{2}{\alpha}}I^{-\frac{2}{\alpha}}}{P^{-\frac{2}{\alpha}}(1-\beta)^{-\frac{2}{\alpha}}}\Gamma\left(1+\frac{2}{\alpha}\right)\right]. \tag{3.57}$$

Now we have simplified the inner expectation and eq. (3.45) can be now be written as

$$= \mathbb{E}\left[\mathbb{1}\left(\frac{M(\Psi)}{I-M(\Psi)} < T\right)\exp\left(-T^{-\frac{2}{\alpha}}I^{-\frac{2}{\alpha}}P^{\frac{2}{\alpha}}(1-\beta)^{\frac{2}{\alpha}}\Gamma\left(1+\frac{2}{\alpha}\right)\right)\right]. \tag{3.58}$$

Using $A = T^{-\frac{2}{\alpha}}P^{\frac{2}{\alpha}}(1-\beta)^{\frac{2}{\alpha}}\Gamma\left(1+\frac{2}{\alpha}\right)$, here it can easily be shown that $\lim_{\beta\to 1}(A) = 0 \Rightarrow \exp(-AI^{-2/\alpha}) = 0$, which shows that all the BSs in the network are transmitting. Above equation can now be written as

$$= \mathbb{E}\left[\mathbb{1}\left(\frac{M(\Psi)}{I-M(\Psi)} < T\right)\exp\left(-AI^{-\frac{2}{\alpha}}\right)\right]. \tag{3.59}$$

Now using the Taylor series expansion of $\exp\left(-AI^{-\frac{2}{\alpha}}\right)$ and exchanging the infinite summation and expectation we have following result

$$1 - \mathsf{P}_c = \sum_{m=0}^{\infty}\frac{(-A)^m}{m!}\mathbb{E}\left[\mathbb{1}\left(\frac{M(\Psi)}{I-M(\Psi)} < T\right)I^{\frac{-2m}{\alpha}}\right]. \tag{3.60}$$

Now the summation can be split as

$$1 - \mathsf{P}_c = \mathbb{E}\left[\mathbb{1}\left(\frac{M(\Psi)}{I-M(\Psi)} < T\right)\right] + \sum_{m=1}^{\infty}\frac{(-A)^m}{m!}\mathbb{E}\left[\mathcal{T}^m\right], \tag{3.61}$$

where $\mathbb{E}\left[\mathcal{T}^m\right] = \mathbb{E}\left[\mathbb{1}\left(\frac{M(\Psi)}{I-M(\Psi)} < T\right)I^{\frac{-2m}{\alpha}}\right]$. For $\tau = (a < b)$ be an event we have $\mathbb{E}(\mathbb{1}_\tau) = \mathbb{P}(a < b)$, using this fact the first term of above equation can now be written as

$$1 - \mathsf{P}_c = \mathbb{P}\left(\frac{M(\Psi)}{I-M(\Psi)} < T\right) + \sum_{m=1}^{\infty}\frac{(-A)^m}{m!}\mathbb{E}\left[\mathcal{T}^m\right]. \tag{3.62}$$

Here it can be observed that the term $1 - \mathbb{P}\left(\frac{M(\Psi)}{I - M(\Psi)} < T\right)$ is the coverage probability for the set of active transmitters in the network. The expression for this coverage probability is given in eq (3.30). Below we provide the solution of $\mathbb{E}\left[\mathcal{T}^m\right]$ which is given by

$$\mathbb{E}\left[\mathcal{T}^m\right] = \mathbb{E}\left[\mathbb{1}\left(\frac{M(\Psi)}{I - M(\Psi)} < T\right) I^{\frac{-2m}{\alpha}}\right]. \tag{3.63}$$

Being consistent with the definition of $\Gamma(x)$ we can express $I^{-2m/\alpha}$ as

$$\Gamma\left(\frac{2m}{\alpha}\right) = \int_0^\infty e^{-sI}(sI)^{\frac{2m}{\alpha}-1}ds \;, m \geq 1, \tag{3.64}$$

after re-arranging the terms we have

$$I^{-\frac{2m}{\alpha}} = \frac{1}{\Gamma(2m/\alpha)}\int_0^\infty e^{-sI}(s)^{\frac{2m}{\alpha}-1}ds \;, m \geq 1. \tag{3.65}$$

Now using this definition of $I^{-\frac{2m}{\alpha}}$ we can write eq. (3.63) as

$$\mathbb{E}\left[\mathcal{T}^m\right] = \mathbb{E}\left[\mathbb{1}\left(\frac{M(\Psi)}{I - M(\Psi)} < T\right)\frac{1}{\Gamma(2m/\alpha)}\int_0^\infty e^{-sI}(s)^{\frac{2m}{\alpha}-1}ds\right]. \tag{3.66}$$

We can exchange the expectation and inner integral which is permissible due to Fubini's theorem, now we have

$$\mathbb{E}\left[\mathcal{T}^m\right] = \frac{1}{\Gamma(2m/\alpha)}\int_0^\infty (s)^{\frac{2m}{\alpha}-1}\mathbb{E}\left[e^{-sI}\mathbb{1}\left(\frac{M(\Psi)}{I - M(\Psi)} < T\right)\right]ds. \tag{3.67}$$

Using the assumption that $T > 1$, at most one BS in the network will be able to connect to the typical user. The indicator function in above equation can now be written as

$$\mathbb{1}\left(\frac{M(\Psi)}{I - M(\Psi)} < T\right) = 1 - \sum_{x \in \Psi}\mathbb{1}\left(\mathsf{SIR}(x) > T\right). \tag{3.68}$$

Now the expectation term in eq. (3.67) can now be written as

$$\mathbb{E}\left[e^{-sI}\mathbb{1}\left(\frac{M(\Psi)}{I - M(\Psi)} < T\right)\right] = \mathbb{E}\left[e^{-sI}\left(1 - \sum_{x \in \Psi}\mathbb{1}\left(\mathsf{SIR}(x) > T\right)\right)\right]. \tag{3.69}$$

Using the fact that $\mathbb{E}(a + b) = \mathbb{E}(a) + \mathbb{E}(b)$, we can write the above equation as

$$\mathbb{E}\left[e^{-sI}\mathbb{1}\left(\frac{M(\Psi)}{I - M(\Psi)} < T\right)\right] = \mathbb{E}\left[e^{-sI}\right] - \mathbb{E}\left[e^{-sI}\sum_{x\in\Psi}\mathbb{1}\left(\mathsf{SIR}(x) > T\right)\right]. \qquad (3.70)$$

It should be noted here that the first term in above equation correspond to the fact that mobile is connected to idle BS set, for this case I act as an interference power. The Laplace transform of interference is given by Theorem 1.

To evaluate the expectation in second term of eq. (3.70) we first represent the effective interference as $I' = I - Ph_{x_o}|x_o|^{-\alpha}$. Now the expectation can be written as

$$= \mathbb{E}\left[e^{-s(I'+Ph_x|x|^{-\alpha})}\sum_{x\in\Psi}\mathbb{1}\left(\frac{Ph_x|x|^{-\alpha}}{I'} > T\right)\right]. \qquad (3.71)$$

In the above equation the expectation is with respect to three random variables which are I', h_x and $|x|$. Since all the random variables are independent we can re-write the equation as follows:

$$= \mathbb{E}_x\left[\sum_{x\in\Psi}\mathbb{E}_{I'}\left[e^{-sI'}\mathbb{E}_{h_x}\left[e^{-sPh_x|x|^{-\alpha}}\mathbb{1}\left(h_x > TI'P^{-1}|x|^{\alpha}\right)\right]\right]\right]. \qquad (3.72)$$

Expectation with respect to h_x can be solved using the fact that $h \sim \exp(1)$ as follows:

$$= \mathbb{E}_{h_x}\left[e^{-sPh_x|x|^{-\alpha}}\mathbb{1}\left(h_x > TI'P^{-1}|x|^{\alpha}\right)\right] \qquad (3.73)$$

$$= \mathbb{E}_{h_x}\left[e^{-sPh_x|x|^{-\alpha}}e^{-TI'P^{-1}|x|^{\alpha}}\right] \qquad (3.74)$$

$$= \frac{e^{-TI'P^{-1}|x|^{\alpha}}}{1 + sP|x|^{-\alpha}}. \qquad (3.75)$$

Now eq. (3.72) can be simplified as

$$= \mathbb{E}_x\left[\sum_{x\in\Psi}\frac{\mathbb{E}_{I'}\left[\exp\left(-I'\left(s + TP^{-1}|x|^{\alpha}\right)\right)\right]}{1 + sP|x|^{-\alpha}}\right]. \qquad (3.76)$$

Here it is observed that $\mathbb{E}_{I'}(.)$ is the Laplace transform of interference evaluated at

$(s + TP^{-1}|x|^{\alpha})$, so we can write above equation as

$$= \mathbb{E}_x \left[\sum_{x \in \Psi} \frac{\mathcal{L}_{I'}\left(s + TP^{-1}|x|^{\alpha}\right)}{1 + sP|x|^{-\alpha}} \right]. \tag{3.77}$$

Now using Campbell's theorem we have the following result

$$= K(x, x) \int_{\mathbb{R}^{\not{2}}} \frac{\mathcal{L}_{I'}\left(s + TP^{-1}|x|^{\alpha}\right)}{1 + sP|x|^{-\alpha}} dx. \tag{3.78}$$

With this we have simplified both terms of eq. (3.70). Now we can write eq. (3.70) as

$$\mathbb{E}\left[e^{-sI}\mathbb{1}\left(\frac{M(\Psi)}{I - M(\Psi)} < T \right) \right] = \mathcal{L}_I(s) - K(x, x) \int_{\mathbb{R}^2} \frac{\mathcal{L}_I\left(s + TP^{-1}|x|^{\alpha}\right)}{1 + sP|x|^{-\alpha}} dx. \tag{3.79}$$

Putting the above result in eq. (3.67) we get

$$\mathbb{E}\left[\mathcal{T}^m \right] = \frac{1}{\Gamma(2m/\alpha)} \int_0^{\infty} (s)^{\frac{2m}{\alpha}-1} \left(\mathcal{L}_I(s) - K(x, x) \int_{\mathbb{R}^2} \frac{\mathcal{L}_I\left(s + TP^{-1}|x|^{\alpha}\right)}{1 + sP|x|^{-\alpha}} dx \right) ds. \tag{3.80}$$

Now the coverage probability form eq. (3.61), after rearranging the terms can be written as

$$\mathsf{P}_c = \left\{ 1 - \mathbb{E}\left[\mathbb{1}\left(\frac{M(\Psi)}{I - M(\Psi)} < T \right) \right] \right\} - \sum_{m=1}^{\infty} \frac{(-A)^m}{m!} \mathbb{E}\left[\mathcal{T}^m \right]. \tag{3.81}$$

By putting the values of $1 - \mathbb{E}\left[\mathbb{1}\left(\frac{M(\Psi)}{I - M(\Psi)} < T \right) \right]$ and $\mathbb{E}\left[\mathcal{T}^m \right]$ from eq. (3.30) and eq. (3.80), respectively, in the above equation we retrieve the final result. $\qquad\square$

Here, it can be seen that the final expression of Theorem 2 involves the computation of integrals and infinite summation. This expression can be evaluated using numerical techniques in MatLab.

3.7   Conclusion

In this chapter, we have incorporated the flexible notion of BS load in a GPP configured single tier cellular network using the idea of conditionally thinning the interference field, conditional on the connection of typical user to its serving BS. Under this setup we found the computable integrable expression for the coverage probability under some mild assumptions. We have also shown that when all the BSs in the network transmit with the probability 1, then the expression for coverage probability reverts back to the case of

fully loaded scenario. Although the expression provided in this chapter for the coverage probability involve long integrals but they can be solved using simple numerical integration techniques. In order to derive the expression for coverage probability in load-aware scenario we also provided the upper bound on the expression of the Laplace transform of interference in a GPP configured network.

Chapter 4

Modelling Multi-Tier Cellular Networks

4.1 Introduction

As mentioned in Chapter 1 the traditional way of increasing the network capacity will not be able to meet the demands of users by 2020. The ultimate solution is the addition of low-powered small cells overlaid to an already existing cellular network to increase the area spectral efficiency [52].While providing increased spectral efficiency, the addition of small cells may increase in-band interference, leading to a drastic degradation in the overall network performance. Understanding the spatial interference patterns in multi-tier cellular networks is of great importance.

Initial efforts in understanding multi-tier cellular networks involved extensive simulations based on the assumptions that macro-cells are fixed on a hexagon grid structure and small cells are uniformly distributed within the coverage area of macro-cell. However, with the addition of more simulation parameters these simulations required too much time and cannot be applied to general scenarios [11]. In order to reduce the dependence on simulations, analytical models based on the PPs are still under the process of investigation in the research literature [8], [12], [53], and [54].

In this chapter we provide a numerical analysis for multi-tier cellular networks, where each tier of the network is modelled using β-GPP, with different values of β. In order to justify our system model we also provide fitness results of β-GPPs to that of actual data set.

4.2   Related Work

The idea of modelling a multi-tier cellular networks via PPs was first given by [8], where the authors provided a base-line model for the analysis of K-tier cellular networks. This work assumed K tiers of networks in which the locations of BSs in each tier was modelled by PPP. The authors in this work computed the coverage probability, the achievable rate and the average load per tier for unbiased cell association. Similarly [55] provided a detailed analysis on the distribution of downlink SINR where different tiers were modelled using PPPs. The work of [8] was further extended to the case of flexible cell association in [53] where the authors found the expression for average ergodic rate and minimum average throughput for the typical user. In [47], the authors incorporated the notion of BS activity factor in the analysis of K-tier cellular network to model the load of each tier, this work also used the PPP assumption for BS locations.

The PPP is one of the most widely used model for the location of BS in the multi-tier cellular networks and have made significant advances from analytical point of view. The independence assumption for the locations of small cells can be justified by the fact that these cells are normally deployed by the end user without any careful frequency planning, but for macro-cells, owned by an operator, the independence assumption is not valid. The PPP model fails to accurately capture the real world deployment scenario for macro-BS since BS are spatially correlated. Accurate models, in which the macro-BS are distributed via some repulsive point process and small cells via irregular or clustered process are still desirable. In [56], an effort has been made to summarize the repulsive and attractive point process that can be used to model various scenarios in multi-tier cellular networks. Recently the authors in [54] have proposed two new models for multi-tier cellular networks. In model 1, the macro BSs are distributed via PPP and pico-BSs via a Poisson hole process [14]. In model 2, the macro BSs and pico BSs follows a PPP and Matern cluster process, respectively. In [51], the model based on βGPP is provided in which each network tier is modelled via tuning the parameter β e.g. macro-BSs locations can be modelled via $\beta \approx 1$ whereas small cell locations by using $\beta \to 0$. The authors in this work provided the coverage probability for the typical user.
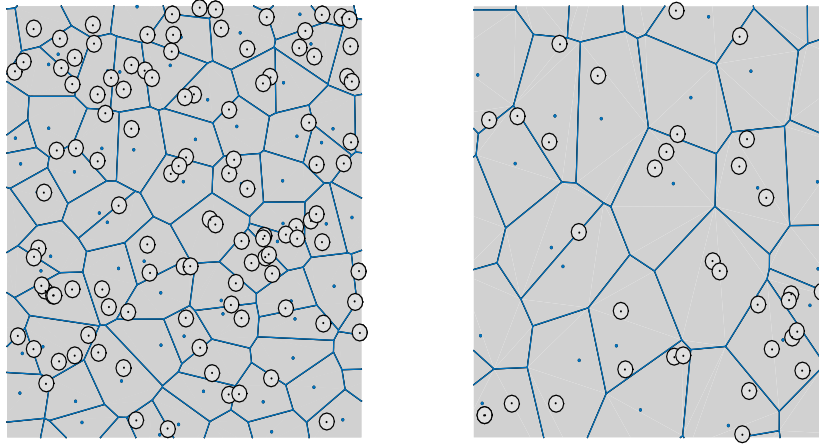
Figure 4.1: Coverage regions in a two-tier cellular network where macro BS locations are taken from β-GPP (with $\beta \approx 1$), the location of small cells also takes the realization of β-GPP (with $\beta \approx 0$). Blue lines and dots represent the coverage region and location of BSs respectively. Small circles represent the coverage area of small cells with the centre being the location of a BS. (Left) Overall view. (Right) Close-up view.

4.3   System Model

We model a two-tier cellular network with macro and femto BSs. Like chapter 3, the locations of macro-BSs are distributed via β-GPP with the value of $\beta \approx 1$ whereas the femto-BSs also takes on the realization of β-GPP but with the value of $\beta \approx 0$ i.e they are irregular. The intensity of femto-BSs is taken as $8\times$ that of macro-BS [8]. The channel model assumed here is simple Rayleigh fading channel and distance based path loss with path loss exponent α. The typical mobile user is connected to the nearest BS, and the connectivity threshold T is assumed to be same for both of the tiers. For numerical analysis the transmit power of macro and femto BSs are taken as $50\,W$ and $0.2\,W$, which are consistent with LTE standard [57].

4.3.1   Coverage Regions

Figure 4.1 shows the coverage regions for the system model for a simulation realisation. These coverage regions can be visually plotted in two steps. First we distribute the macro-BSs using a β-GPP in the specific area and the whole area is then tessellated using the maximum SIR connectivity model[1]. Here it should be noted that in reality the BSs

---

[1]In Matlab we have used the command voronoi to plot this area

Figure 4.2: Distribution of BSs in the urban region of United Kingdom. Total number of BSs are 161 in the region of $2 \times 1.8 \, \text{km}^2$ region. Red triangles represent the locations of BSs. (Left:) Overall view. (Right:) Close up view.

coverage regions are fuzzy because of fading. Therefore, these coverage regions can be assumed as average coverage footprints over a period of time so that the effect of fading is averaged out. The coverage footprints of femto-BSs are simply the small circles since they are transmitting with much less power.

4.4   Fitting a Point Process to an Actual Data Set

In order to test the goodness-of-fit of a PP to any data set, various summary statistics can be used which are explained in Section 2.5.2. In the case of wireless networks, the more practical performance metric is coverage probability i.e., $\mathsf{P}_c(T)$ (T is the SINR threshold), to test the goodness-of-fit. In this section we provide the modelling accuracy of the β-GPP to publicly available data set for a single-tier cellular networks, obtained from Ofcom[2]. This same data set is the one that has been used by most of the current research in stochastic geometry (e.g. [27] and [58]). Figure 4.2 shows the location of BSs of Vodafone operator in 2×1.8 km urban region in United Kingdom. The total number of BS lying in this region are 161, thus leading to the computation of intensity λ as $\frac{Number\ of\ BSs}{Total\ Region} = 3.142$ km^{-2}. The probability of coverage $\mathsf{P}_c(T)$ for actual data is computed numerically by determining the covered area fraction for $\mathsf{SINR} > T$. In our simulations, we have neglected the noise power since it is negligible as compared to the interference. So, instead of

---

[2]The independent regulatory authority for the UK communications industries, where the data is open to the public. Website: http://www.sitefinder.ofcom.org.uk/
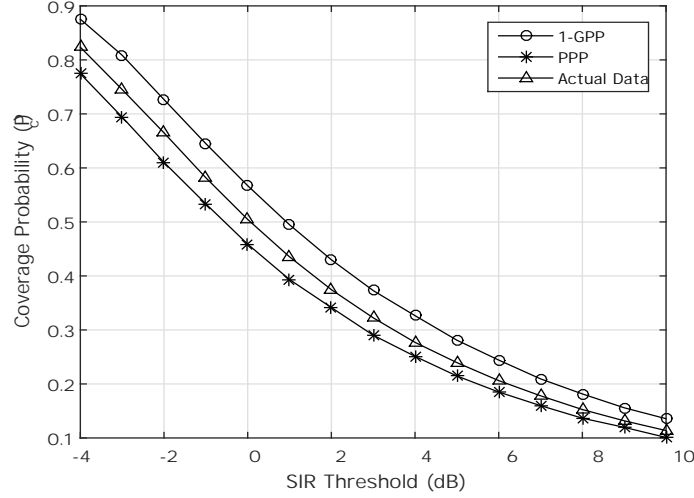
Figure 4.3: Fitting results based on the coverage probability of GPP and PPP to an actual BS data set of urban region ($\alpha = 3$ and $P = 50W$).

computing SINR we have computed the SIR at 10^5 different random location within the finite region using Monte Carlo simulations. The simulation time was approximately 5 minutes using Matlab on a standard desktop computer. One thing to be noted here is that we have provided the result for only $\alpha = 3$, because for the lower values of α most of the interference comes from the far-away transmitter which in this case are not present since we are dealing with a finite area. Furthermore, in order to avoid the boundary effect we use only the central area to get the values of SIR.

Here, we have also provided the fitting-results for the PPP (where the location of BSs are taken from the PPP). As it can be seen from Figure 4.3 that actual BS data set is much regular than PPP but still less regular than 1-GPP, since the curve for the 1-GPP lies above the curve of actual BS data set. But, in case of β-GPP we can control the regularity of points by tuning the parameter β. Figure 4.4 provide the fitting results for different values of β with actual data set. Here we found that the value of $\beta = 0.8$ gives the perfect fit for our selected data set in urban region.

4.5   Load Aware Modelling in Multi-tier Cellular Networks

For the system model described in section 4.3 we introduce the notion of BS load and provide numerical results for coverage probability in this section. As argued in the
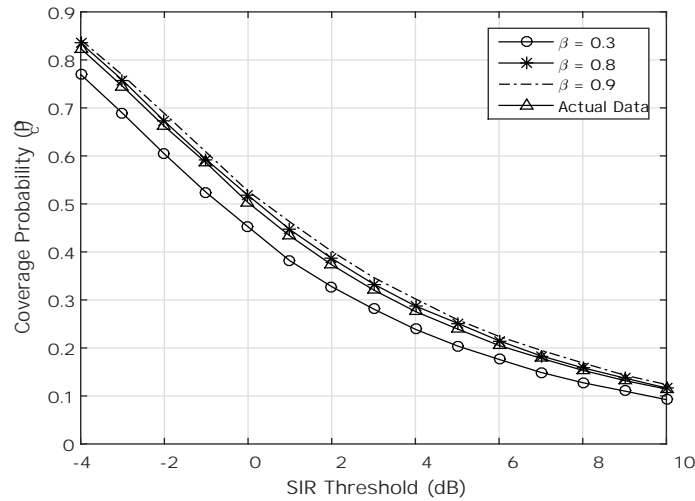
Figure 4.4: Fitting results based on the coverage probability of β-GPP to an actual BS data set of urban region with different values of β ($\alpha = 3$ and $P = 50W$).

previous chapter all the macro-BSs do not transmit at all times. Same is the case with the femto-BSs since small cells are user-owned (serving on average 3-4 users at a time) and are not active all times. Figure 4.5 shows the coverage probability comparison of the full load scenario with that of load aware. In this analysis the macro-BSs transmit with a probability of 0.8 whereas femto-BSs are transmitting with the probability 0.6. The ratio between the powers of macro-BSs to femto-BSs is set to 25, i.e., macro-BSs are transmitting with $25\times$ more power as that of femto-BS. It can be observed easily, when all the BSs are not transmitting at all times, the coverage probability increases.

4.6   Access Policies for Small Cells

Our previous analysis is based on the open access policy where a user can connect to any small cell in the whole network. In this section we study the impact of closed-access policy on the coverage probability using Monte Carlo simulations. Developing the analytical model for closed-access policy with β-GPP deployed BSs is a promising future research direction.

4.6.1   Closed Access

To study the effect of closed access policy of small cells, we consider a two-tier cellular network as mentioned in Section 4.3. The typical user can connect to any macro-BS in the whole network since they are operator owned to provide the services to the user. To model
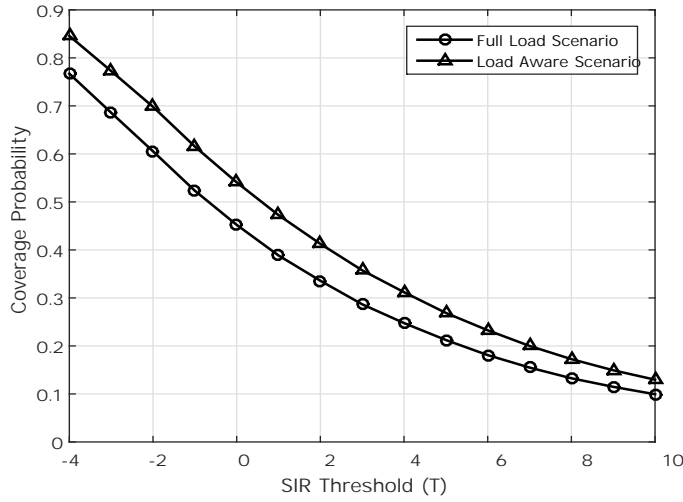
Figure 4.5: The coverage probability comparison of full load and load aware scenario $(\alpha = 3)$.

the CSGs for small cells, a typical user can connect to small cell with the probability τ independently. For an overall intensity λ of small cells, the intensity of open-access small cells is given by $\lambda_o = \tau \lambda$, and intensity of closed-access small cells is given by $\lambda_c = (1-\tau)\lambda$. The overall intensity is

$$\lambda = \tau \lambda + (1 - \tau)\lambda. \tag{4.1}$$

Under these assumptions we compute the coverage probability for different values of τ. It can easily be seen from Figure 4.6 that with an increasing value of τ the coverage probability also increases. The analysis provided here should not be confused with the analysis provided earlier, since in this case mobile user may not be able to connect to the small cell but still gets the interference from that particular small cell. Whereas, in the previous analysis the silent BS does not contribute to interference since it is not transmitting at that particular time instant.

The curves provided in Figure 4.6 can be divided in two parts: 1) higher SIR regimes (greater than 0 dB), 2)lower SIR regimes (less than 0 dB). A specific user normally enjoy the high SIR at the center of the cell. It is evident from the coverage analysis curve that if the user is at the center of the cell then access policy of small cell do not affect the coverage probability too much. However at the cell edges, i.e., in low SIR regimes, a user get affected due to the closed accessed policy. In order the maintain the balance in coverage region across the service area, the cellular network operators should install the small cells with open access policy at the cell edges.
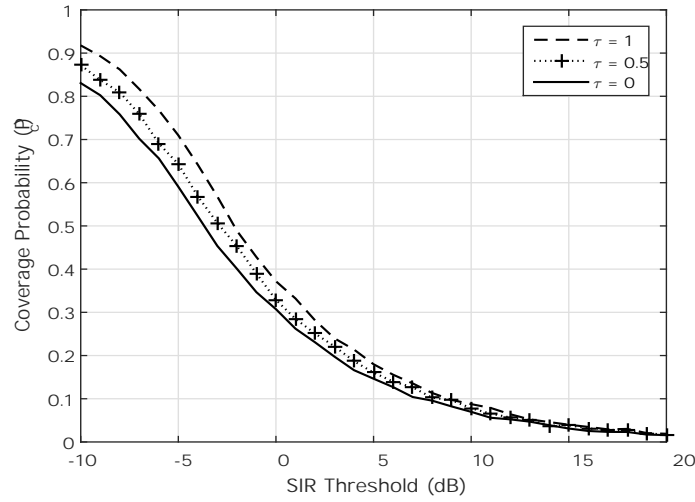
Figure 4.6: The coverage probability in two-tier cellular network ($\alpha = 4$), with different values of access probability. The ratio between powers of macro to femto BSs is set to 25.

4.7   Conclusion

In this chapter, we modelled a two-tier cellular network with β-GPP where the value of β for macro-BS locations is set to 0.8 due to regularity. For this model we provide the coverage probability curve with full load and load aware scenarios. Here we also incorporated the access policies of small cells to the system. Based on our analysis, we determined that closed access policy degrades the overall coverage probability of the network but at lower SIR regimes. This is because of the fact that small cells, in our case femto cells, transmit with much less power as compared to macro-BSs and therefore, they do not contribute too much to the interference in high interference regimes. In the case that the femto cells are installed at the cell edge then the access policy would definitely degrade the overall performance of the network.

To demonstrate the accuracy and practicability of β-GPPs for wireless networks, we fitted the point process model to a publicly available data set using coverage probability as a performance metric. The fitting results revealed that the different regions of actual BS deployment can be modelled by simply tuning the parameter β, e.g., urban scenarios can be modelled with high values of β.

Chapter 5

Conclusion and Future Work

This thesis, at first, provides an overview of the PPs that can be used for the modelling of wireless networks. Repulsive PPs provide the best fit for macro base station (BS) positions in cellular networks whereas attractive point processes can be used to model small cell positions. A brief overview of the tools from stochastic geometry is also provided which are used for the mathematical analysis of PPs.

Keeping in view the trade-off between analytical tractability, accuracy and practicability of the point processes we have employed the β-Ginibre point process (β-GPP) to capture the underlying separation between the BSs of multi-tier cellular networks. To show the analytical tractability of the β-GPP model we derived the computable integral upper bound on the Laplace transform of interference for a single-tier cellular network. Apart from using the accurate model for the locations of BSs we have addressed the issue of BS load in our analysis. In the practical scenario, all the BSs do not transmit simultaneously at all the time, this may not be true for the peak hours but, generally, some BSs in the network remain silent in a specific time slot. We have incorporated the concept of *conditional thinning* of interference field in the network. Conditioned on the connection of the typical mobile to its serving BS all the BSs in the network transmit independently with probability β. Under this setting, we derived the approximate expression for the coverage probability of typical user. The comparison of fully loaded with that of load-aware β-GPP single-tier cellular network model revealed that fully loaded scenario is extremely pessimistic in terms of coverage probability.

In order to demonstrate the accuracy of the model we have fitted the β-GPP, using the coverage probability, to publicly available data of BS deployment. Based on our analysis we found that the β-GPP with $\beta \approx 1$ is an accurate model for the location of BSs of macro-cells. However, values of $\beta \approx 0$ provides the best fit for the location of small cells due to their unplanned nature of deployment. So, by carefully adjusting the parameter β

we can model different tiers of the multi-tier cellular networks. In our case, the value of $\beta = 0.8$ provides the best fit for the selected BS data set of an urban region.

We have extended our analysis to the case of two-tier cellular networks where we have used β-GPP to for different tiers by adjusting the parameter β. Through Monte Carlo simulations we have provided the coverage probability analysis for both the full load and load ware scenarios. Apart from this, the effect of small cells access policies on the spatial distribution of interference was also investigated. In this direction, we found that closed access policy do not affect the cell center users that much as the cell edge users.

This work has numerous extensions, the most promising future directions are as follows:

Analysis of Multi-tier cellular network: Through simulations, by tuning the parameter β we have shown that different tiers of multi-tier network can be modelled. At the same time, the mathematical analysis provided here is for the single-tier cellular network. The first and foremost direction is to extend the same load-aware analysis for the multi-tier cellular network. Recently [51] has derived the expressions for the coverage probability in which all the tiers are distributed via β-GPP assuming the fully loaded scenario. However, we are aiming at incorporating the notion of BS load in the analysis, since, in case of multi-tier network, small cells do not transmit at all the times even during the peak traffic hours. The second most important aspect is the access policy of small cells. The mobile user may not be able to connect to the strongest base station due to a closed access policy but is still getting interference from that small cell. So understanding the interference patterns under different access policies using β-GPP model is of great importance. In this direction, we are quite optimistic that we will be able to answer questions like: *What effect would access policy have on the overall distribution of interference?, How does the addition of small cells affect the coverage probability and ultimately the data rate achieved?*

Interference Mitigation in Multi-tier Cellular networks: Interference is one of the main performance-limiting factors in the future generation of cellular networks. Most of the research discussion in this direction revolves around the introduction of Coordinated Multi-Point (CoMP) schemes in future releases [59]. The main idea is to increase the data rate of the edge users or the users facing high interference by introducing some coordination in between different BSs. In other words we can say that transforming the

interfering BSs to the cooperating BSs to increase the Signal to Interference Ratio and ultimately the capacity.

After studying the interference footprint in the multi-tier cellular network using β-GPP we would be in strong position to study the cooperating schemes for the mitigation of interference in multi-tier cellular networks. Another promising direction is to study different CoMP schemes keeping in view capacity of the overall network.

Bibliography

[1] A. A. Huurdeman, *The Worldwide History of Telecommunications.* John Wiley & Sons, 2003.

[2] T. S. Rappaport, *Wireless Communications: Principles and Practice.* Prentice-Hall, 2nd ed., 2002.

[3] Cisco, "Visual networking index: Forecast and methodology," tech. rep., White paper at cisco.com, 2014.

[4] U. Doetsch, N. Bayer, H. Droste, A. Roos, T. Rosowski, G. Zimmermann, P. Agyapong, N. F. Lindqvist, I. D. Silva, H. Eriksson, H. Tullberg, O. Bulakci, J. Eichinger, K. Dimtsa, M. Stamatelatos, V. Venkatkumar, M. Boldi, and I. Berberana, "Final report on architecture ict-317669," tech. rep., Mobile and wireless communication Enablers for Twenty-twenty Information Society (METIS), 2015.

[5] J. G. Andrews, S. Buzzi, W. Choi, S. Hanly, A. Lozana, A. C. Soong, , and J. C. Zhang, "What will 5g be?," *IEEE Journal on Selected Areas in Communications*, vol. 32, pp. 1065–1082, Jul. 2014.

[6] V. Jungnlckel, K. Manolakis, W. Zirwas, B. Panzner, V. Braun, M. Lossow, M. Stemad, R. Apelfrojo, and T. Svensson, "The role of small cells, coordinated multipoint, and massive mimo in 5g," *IEEE Communications Magazine*, vol. 52, no. 5, pp. 44–51, 2014.

[7] P. Lin, J. Zhang, and Q. Zhang, "Macro-femto heteregeneous network deployment and management: From business models to technical solutions," *IEEE Wireless Communications*, vol. 18, pp. 64–70, June 2011.

[8] H. S. Dhillon, R. K. Ganti, F. Baccelli, and J. G. Andrews, "Modelling and analysis of k-tier downlink heterogeneous cellular networks," *IEEE Journal on Selected Areas in Communications*, vol. 30, pp. 550–560, Apr. 2012.

[9] J. G. Andrews, H. Claussen, M. Dohler, S. Rangan, and M. C. Reed, "Femtocells: Past, present and future," *IEEE Journal on Selected Areas in Communications*, vol. 30, no. 3, pp. 497–508, 2012.

[10] V. Chandrasekhar and J. G. Andrews, "Femtocell networks: A survey," *IEEE Communications Magazine*, vol. 46, pp. 59–67, Sep. 2008.

[11] S. Mukherjee, *Analytic Modeling of Heteregeneous Cellular Networks Geometry, Coverage and Capacity.* Cambridge University Press, 2014.

[12] J. G. Andrews, F. Baccelli, and R. K. Ganti, "A tractable approach to coverage and rate in cellular networks," *IEEE Transaction on Communications*, vol. 59, pp. 3122–3134, Nov. 2011.

[13] S. N. Chiu, D. Stoyan, W. S. Kendall, and J. Mecke, *Stochastic Geometry and its Applications.* Wiley Series in Probability and Statistics, 3 ed., 2013.

[14] M. Haenggi, *Stochastic Geometry for Wireless Networks.* Cambridge University Press, 2012.

[15] F. Baccelli and B. Blaszczyszyn, *Stochastic Geometry and Wireless Networks, Volume I - Theory*, vol. 1. NoW Publishers, 2009.

[16] M. H. R. Ganti, *Interference in Large Wireless Networks, in Foundations and Trends in Networking.* NOW Publishers, 2008.

[17] S. P. Weber and J. G. Andrews, *Transmission Capacity of Wireless Networks, in Foundations and Trends in Networking.* NOW Publishers, 2012.

[18] Z. Khalid and S. Durrani, "Distance distributions in regular polygons," *IEEE Transaction on Vehicular Technology*, vol. 62, pp. 2363–2368, June 2013.

[19] M. Haenggi, "Mean interference in hard-core wireless networks," *IEEE Communication Letters*, vol. 15, pp. 792–794, Aug 2011.

[20] A. Guo and M. Haenggi, "Spatial stochastic models and metrics for the structure of base station in cellular networks," *IEEE Transaction on Wireless Communications*, vol. 12, pp. 5800–5812, Nov. 2013.

[21] O. Macchi, "The coincidence approach to stochastic point processes," *Advances in Applied Probability*, pp. 83–122, 1975.

[22] F. Lavancier, J. Moller, and E. Rubak, "Determinantal point process models and statistical inference extended version," *To appear in Journal of the Royal Statistical Society, series B*, 2015.

[23] C. Biscio and F. Lavancier, "Quatifying repulsiveness of determinantal point processes," *arXiv preprint:arXiv:1406.2796*, Dec. 2014.

[24] J. B. Hough, M. Krishnapur, Y. Peres, and B. Viràg, *Zeros of Gaussian Analytic Functions and Determinantal Point Processes.* American Mathematical Society, 2009.

[25] J. Ginibre, "Statistical ensembles of complex, quaternion, and real matrices," *Journal of Mathematical Physics*, vol. 6, pp. 440–449, Mar. 1965.

[26] I. Camilier and L. Decreusefond, "Quasi-invariance and integration by parts for determinantal and permanental processes," *Journal of Functional Analysis*, vol. 259, pp. 268–300, 2010.

[27] N. Deng, W. Zhou, and M. Haenggi, "The ginibre point process as a model for wireless networks with repulsion," *IEEE Transaction on Wireless Communications*, vol. 14, pp. 107–121, Jan. 2015.

[28] E. Kostlan, "On the spectra of gaussian matrices," *Linear Algebra and its Applications*, vol. 162-164, pp. 385–388, 1992.

[29] J. B. Hough, M. Krishnapur, Y. Peres, and B. Viràg, "Determinantal processes and independence," *Probability Surveys*, vol. 3, pp. 206–229, 2006.

[30] A. Baddeley and R. Turner, "spatstat: An r package for analyzing spatial point patterns," *Journal of Statistical Software*, vol. 12, pp. 1–42, January 2005.

[31] L. Decreusefond, I. Flint, and A. Vergne, "Efficient simulation of ginibre point process," *Journal of Applied Probability, Applied Probability Trust*, vol. 54, no. 4, 2015.

[32] M. Haenggi, "On distances in uniformly random networks," *IEEE Transaction on Information Theory*, vol. 51, pp. 3584–3586, October 2005.

[33] B. D. Ripley, *Spatial Statistics*. John Wiley & Sons, second ed., 1981.

[34] Y. Li, F. Baccelli, H. S. Dhillon, and J. G. Andrews, "Statistical modelling and probabilistic analysis of cellular networks with determinantal point processes," *arXiv preprint: arXiv:1412.2087v1*, Dec. 2014.

[35] T. Shirai and Y. Takahashi, "Random point fields assiciated with certain fredholm determinants i: fermion, poisson and boson point processes," *Journal of Functional Analysis*, vol. 205, pp. 441–463, April 2003.

[36] C. E. Shanon, "A mathematical theory of communication," *Bell System Technical Journal*, vol. 27, pp. 379–423,623–656, Jul., Oct. 1948.

[37] L. Chen, W. Chen, B. Wang, X. Zhang, H. Chen, and D. Yang, "System-level simulation methodology and platform for mobile cellular systems," *IEEE Communications Magazine*, vol. 49, pp. 148–155, Jul. 2011.

[38] K. B. Baltzis, "A geometrical based model for cochannel interference analysis and capacity estimation of cdma cellular system," *EURASIP Journal on Wireless Communications and Networking*, 2008.

[39] P. Petrus, R. B. Etrel, and J. H. Reed, "Capacity enhancement using addaptive arrays in an amps system," *IEEE Transaction on Vehicular Technology*, vol. 47, pp. 717–727, Aug. 1998.

[40] M. Haenggi, J. G. Andrews, F. Bacelli, O. Douse, and M. Franceschetti, "Stochastic geometry and random graphs for the analysis and design of wireless networks," *IEEE Journal on Selected Areas in Communications*, vol. 27, no. 7, pp. 1029–1046, 2009.

[41] F. Baccelli, M. Klein, M. Lebourges, and S. Zuyev, "Stochastic geometry and architechture of communication networks," *Journal on Telecommunication Systems*, vol. 7, no. 1, pp. 209–227, 1997.

[42] S. P. Weber, X. Yang, J. G. Andrews, and G. de Veciana, "Transmission capacity of wireless ad hoc networks with outage constraints," *IEEE Transaction on Information Theory*, vol. 51, pp. 4091–4102, Dec. 2005.

[43] A. Hassan and J. G. Andrews, "The guard zone in wireless ad hoc networks," *IEEE Transaction on Wireless Communications*, vol. 6, pp. 897–906, Mar. 2007.

[44] A. Hassan and A. Ali, "Guard zone based scheduling in ad hoc networks," *Computer Communications*, vol. 56, pp. 89–97, Feb. 2015.

[45] N. Miyoshi and T. Shirai, "A cellular network model with ginibre configured base stations," *Research Report on Mathematical and Computing Sciences*, vol. 46, pp. 832–845, Jun. 2012.

[46] N. Miyoshi and T. Shirai, "Downlink coverage probability in cellular networks with ginibre deployed base stations and nakagami-m fading channel," in *13th International Symposium on Modelling and Optimization in Mobile, Ad Hoc and Wireless Networks (WiOpt)*, 2015.

[47] H. S. Dhillon, R. K. Ganti, and J. G. Andrews, "Load-aware modeling and analysis of heterogeneous cellular networks," *IEEE Transaction on Wireless Communications*, vol. 12, pp. 1666–1677, April 2013.

[48] R. Irmer, H. Droste, P. Marsch, M. Grieger, G. Fettweis, S. Brueck, H.-P. Mayer, L. Thiele, and V. Jungnickel, "Coordinated multipoint: Concepts, performance, and field trial results," *IEEE Communications Magazine*, pp. 102–11, Feb. 2011.

[49] I. Ipsen and D. Lee, "Determinant approximations," *arXiv preprint: arxiv:1105.0437*, 2011.

[50] I. S. Gradshteyn and I. M.Ryzhik, *Table of Integrals Series and Products.* New York: Academic Press, 1965.

[51] I. Nakata and N. Miyoshi, "Spatial stochastic models for analysis of heteregeneous cellular networks with repulsively deployed base stations," *Performance Evaluation*, vol. 78, pp. 7–17, 2014.

[52] A. Ghosh, N. Mangalvedhe, R. Ratasuk, B. Mondal, M. Cudak, E. Visotsky, T. A. Thomas, J. G. Andrews, P. Xia, H.-S. Jo, H. S. Dhillon, and T. D. Novlan, "Heterogeneous cellular network: From theory to practice," *IEEE Communications Magazine*, vol. 50, no. 6, pp. 54–64, 2012.

[53] H.-S. Jo, Y. J. Sang, P. Xia, and J. G. Andrews, "Heterogeneous cellular networks with flexible cell association: A comprehensive downlink sinr analysis," *IEEE Transaction on Wireless Communications*, vol. 11, pp. 3484–3495, Oct. 2012.

[54] N. Deng, W. Zhou, and M. Haenggi, "Heterogeneous cellular network models with dependence," *IEEE Journal on Selected Areas in Communications*, vol. to appear, 2015.

[55] S. Mukherjee, "Distribution of downlink sinr in heterogeneous cellular networks," *IEEE Journal on Selected Areas in Communications*, vol. 30, pp. 575–585, April 2012.

[56] Y. J. Chun, M. O. Hasna, and A. Ghrayeb, "Modeling heterogeneous cellular networks interference using poisson cluster processes," *IEEE Journal on Selected Areas in Communications*, vol. to appear, 2015.

[57] A. Ghosh, J. Zhang, J. G. Andrews, and R. Muhamed, *Fundamentals of LTE.* Prentice-Hall, 2010.

[58] L. Wu, Y. Zhong, and W. Zheng, "Spatial statistical modelling for heterogeneous cellular networks - an empirical study," in *IEEE VTC-Spring*, (Seoul, Korea), pp. 1–6, IEEE, May 2014.

[59] E. Hossain, M. Rasti, H. Tabassum, and A. Abdelnasser, "Evolution towards 5g multi-tier cellular wireless networks: An interference management perspective," *IEEE Wireless Communications*, vol. 21, no. 3, pp. 118–127, 2014.